nature biotechnology

Article

https://doi.org/10.1038/s41587-023-01756-1

Efficient engineering of human and mouse primary cells using peptide-assisted genome editing

Received: 3 August 2022

Accepted: 22 March 2023

Published online: 24 April 2023

Check for updates

Zhen Zhang[1,2], Amy E. Baxter[3,4], Diqiu Ren[1,5,6], Kunhua Qin[1,7], Zeyu Chen[3,4], Sierra M. Collins[1,2], Hua Huang[1,2,3], Chad A. Komar[1,5,6], Peter F. Bailer[1,8,9], Jared B. Parker[8], Gerd A. Blobel[1,7], Rahul M. Kohli[1,8,9], E. John Wherry[3,4,10] ✉, Shelley L. Berger[1,2] ✉ & Junwei Shi[1,5,6] ✉

Simple, efficient and well-tolerated delivery of CRISPR genome editing systems into primary cells remains a major challenge. Here we describe an engineered Peptide-Assisted Genome Editing (PAGE) CRISPR–Cas system for rapid and robust editing of primary cells with minimal toxicity. The PAGE system requires only a 30-min incubation with a cell-penetrating Cas9 or Cas12a and a cell-penetrating endosomal escape peptide to achieve robust single and multiplex genome editing. Unlike electroporation-based methods, PAGE gene editing has low cellular toxicity and shows no significant transcriptional perturbation. We demonstrate rapid and efficient editing of primary cells, including human and mouse T cells, as well as human hematopoietic progenitor cells, with editing efficiencies upwards of 98%. PAGE provides a broadly generalizable platform for next-generation genome engineering in primary cells.

RNA-guided CRISPR–Cas genome engineering tools[1–3] have enabled and facilitated numerous new directions in biology and medicine, including understanding the genetic basis of diseases, making precise genetic alterations for gene therapy and engineering cellular therapeutics programmed to reverse disease states. However, to reach their full potential, major advances are necessary in the approaches to deliver CRISPR components specifically to primary cells, those directly isolated from human and animal tissues, in order to unleash the full power of genome editing for basic research, cell engineering and gene therapy.

As one example of the importance of primary cell engineering, T cells serve as central players in viral infection, autoimmunity and immunotherapy for cancer. Adoptive transfer of engineered T cells, such as chimeric antigen receptor (CAR) T cells, has been a major leap forward for immuno-oncology, achieving durable clinical responses in numerous treatment-refractory cancers[4,5]. Advancing the next generation of engineered adoptive T cell therapies relies on effective CRISPR-based genome editing and engineering tools[1–3,6]. Currently, however, efficient delivery of the CRISPR system into primary T cells remains a major challenge, relying heavily on optimizing the use of viral vectors, physical electroporation and/or lipid nanoparticles individually or in combination (Supplementary Fig. 1)[7,8]. Related challenges exist in mouse disease models, where the difficulty of Cas protein delivery

[1]Epigenetics Institute, University of Pennsylvania, Philadelphia, PA, USA. [2]Department of Cell and Developmental Biology, University of Pennsylvania, Philadelphia, PA, USA. [3]Department of Systems Pharmacology and Translational Therapeutics, University of Pennsylvania, Philadelphia, PA, USA. [4]Institute for Immunology and Immune Health, University of Pennsylvania, Philadelphia, PA, USA. [5]Department of Cancer Biology, University of Pennsylvania, Philadelphia, PA, USA. [6]Abramson Family Cancer Research Institute, University of Pennsylvania, Philadelphia, PA, USA. [7]Division of Hematology, The Children's Hospital of Philadelphia, Philadelphia, PA, USA. [8]Department of Medicine, University of Pennsylvania, Philadelphia, PA, USA. [9]Department of Biochemistry and Biophysics, University of Pennsylvania, Philadelphia, PA, USA. [10]Parker Institute for Cancer Immunotherapy, Perelman School of Medicine, University of Pennsylvania, Philadelphia, PA, USA. ✉e-mail: wherry@pennmedicine.upenn.edu; bergers@pennmedicine.upenn.edu; jushi@upenn.edu

https://doi.org/10.1038/s41587-023-01756-1

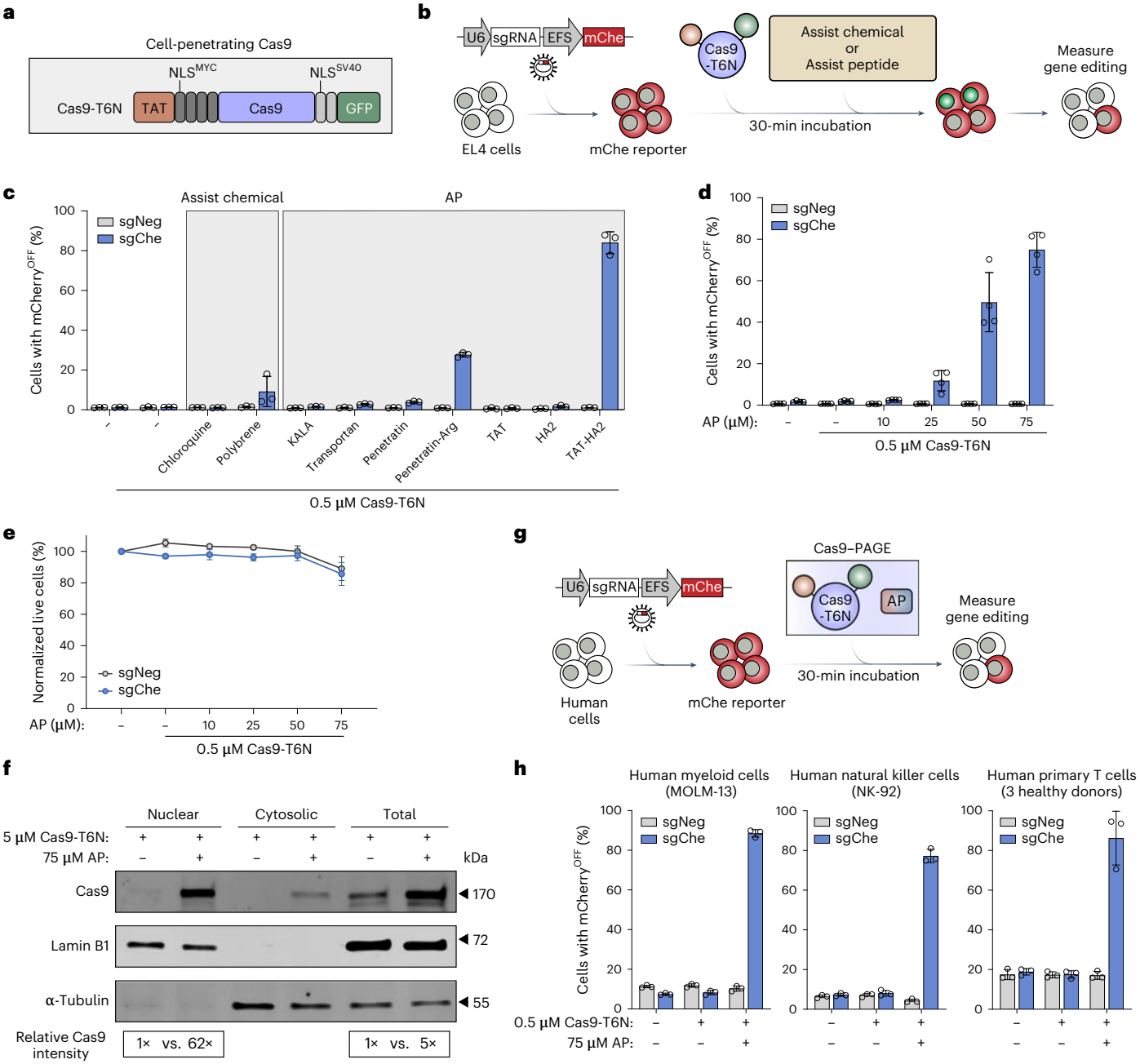

Fig. 1 | Development of PAGE CRISPR–Cas9 system. a, Design of a cell-penetrating Cas9 (Cas9-T6N). Cas9 is fused N-terminally to HIV TAT and 4× Myc NLS and C-terminally to 2× SV40 NLS and GFP. **b**, Schematic workflow to quantify the gene editing efficiency of different Cas9-CPPs and conditions using an EL4 mCherry (mChe) reporter cell. EL4, a mouse T lymphoblast, was lentivirally transduced with a bicistronic expression vector stably expressing an mChe fluorescence reporter and a sgRNA targeting the *mCherry* gene or the *Ano9* gene as a negative control. EL4 mChe cells were incubated with Cas9-T6N protein together with various assist chemicals or APs for 30 min, followed by extensive washing and trypsinization to remove residual cell surface-bound Cas9-T6N. Gene editing efficiency was quantified by the loss of the mChe-positive cell population via flow cytometry. **c**, Quantification of the editing efficiency of Cas9-T6N with various assist chemicals and APs in the EL4 mChe reporter cell line. EL4 mChe reporter cells were treated with 0.5 μM Cas9-T6N in the presence of the chemicals 200 mM chloroquine or 1 mg ml^{-1} polybrene, or 75 μM of the APs as indicated. The percentage of cells with loss of mChe was measured by flow cytometry on day 4 post-treatment ($n = 3$, biological replicates). **d**,**e**, Quantification of gene editing efficiency and live cell recovery with titration of AP. EL4 mChe cells were treated with 0.5 μM Cas9-T6N in the presence of various concentrations of AP, here TAT-HA2. Live cell populations were measured immediately following treatment, while gene editing efficiency was measured at day 4 post-treatment ($n = 4$, biological replicates). **f**, Western blotting of Cas9, lamin B1 and α-Tubulin levels in the nuclear fraction, cytosolic fraction and whole-cell lysates prepared from EL4 cells were incubated with either Cas9-T6N only or Cas9-T6N and TAT-HA2. EL4 cells were incubated with 5 μM of Cas9-T6N ±75 μM of TAT-HA2 for 30 min. Nuclear and cytosolic fractions were separated and subjected to immunoblotting analyses using antibodies against Cas9, nuclear marker lamin B1 and cytosolic marker α-Tubulin. A representative experiment of two independent replicates is shown ($n = 2$, biological replicates). The relative intensity of Cas9 protein is quantified using gel densitometry and normalized first to lamin B1 and then to the Cas9 from either a nuclear fraction or whole-cell lysates without TAT-HA2 treatment. Here AP is TAT-HA2. **g**, Workflow of Cas9-PAGE system for gene editing in diverse human cell types. The combination of cell-penetrating Cas protein and AP was termed PAGE. **h**, Quantification of PAGE system-mediated gene editing efficiency in various human cell types. mChe reporter was established in indicated cell types: a human myeloid cell line MOLM-13, a human natural killer cell line NK-92 and human primary T cells isolated from peripheral blood mononuclear cells of three healthy donors. mChe reporter cells were incubated with 0.5 μM Cas9-T6N and 75 μM AP for 30 min. The percentage of cells with loss of mChe was measured by flow cytometry on day 4 post-treatment ($n = 3$, biological replicates). Error bars smaller than the symbol width were not shown. Data were presented as mean ± s.d.

via viral vectors or other approaches often necessitates a cumbersome and lengthy process of breeding Cas9-expressing transgenic animals to different inducible or lineage-specific strains for genetic studies in vivo[9–13]. Direct delivery of Cas proteins or Cas ribonucleoprotein (RNP) complexes could provide a simple and broadly applicable approach for genome editing in primary T cells.

The direct application of CRISPR–Cas9 nuclease and its associated polyanionic single guide RNA (sgRNA) is limited by poor cellular uptake for a lack of intrinsic cell penetration capability. Prior efforts to enable protein-based direct delivery of the CRISPR system into cells explored several approaches as follows: Cas9 has been linked with negatively-charged GFP and complexed with cationic lipids[14], chemically conjugated and co-incubated with a polyarginine peptide[15] or linked with multiple copies of nuclear localization sequences (NLS)[16]. The latter two approaches using polyarginine peptides and NLS sequences relied on the principle that short cell-penetrating peptides (CPPs) can potentially facilitate the cellular uptake of user-defined molecular cargo through endocytosis[17,18]. Although these prior approaches permitted editing in both mouse and human cell lines, these methods were generally inefficient in primary cell types. The cumulative inefficiencies of multiple cellular localization events—cell entry, escape from the endosome and localization to the nucleus—have thus prohibited the wide adoption of CPP-based CRISPR delivery.

In this study, we engineered a Peptide-Assisted Genome Editing (PAGE) CRISPR–Cas system for facile, efficient, and nontoxic genome editing of primary cells. The PAGE system consists of a cell-penetrating Cas protein, such as Cas9 or Cas12a, as well as a cell-penetrating endosomal escape peptide. With only a 30-min incubation period, the PAGE system can achieve robust gene editing in both Cas protein and Cas RNP complex formats, while generating minimal cellular toxicity and perturbation of gene transcription. We demonstrated the utility of the CRISPR-PAGE system for highly efficient single and multiplex genome editing in human primary T cells and hematopoietic progenitor cells.

Results

Development of PAGE CRISPR–Cas system

We initially considered the hypothesis that alternative CPP and NLS configurations could overcome these existing barriers to CPP-based CRISPR gene engineering. Therefore, we designed and tested purified recombinant Cas9 fusion proteins with diverse CPP and NLS combinations to assist cell penetration and nuclear localization, respectively. We also added a GFP fluorescence marker to enable monitoring of cellular uptake (Fig. 1a and Supplementary Fig. 2). To evaluate the gene editing efficiency of Cas9-CPP variants, we transduced a mouse T lymphoblast cell line, EL4, with an mCherry (mChe) fluorescence reporter co-expressed with either an mChe targeting sgRNA (sgChe) or a negative control sgRNA (sgNeg). The reporter lines provided a quantitative readout of on-target Cas9-mediated indels in the mChe gene, allowing for facile screening of different Cas9-CPPs and conditions (Supplementary Fig. 3a). We transiently incubated various Cas9-CPPs with the reporter cells for 30 min, followed by removal of cell surface-bound protein with trypsin, and assessed gene editing via flow cytometric analysis of the loss of the mChe-positive cell population after 4 d (Supplementary Fig. 3a). Across configurations, negligible editing of mChe was observed using 0.5 μM of each construct (Supplementary Fig. 4a). When employing a tenfold higher concentration (5 μM) of the TAT-4xNLS-Cas9-2xNLS-sfGFP (Cas9-T6N), ~20% cell penetration efficiency was achieved. Coordinately, we observed a ~13% loss of the mChe-positive population only in the cells with sgChe but not in the cells with sgNeg, suggesting the feasibility of measuring on-target Cas9-T6N gene editing (Supplementary Fig. 3b,c). Nonetheless, our results were consistent with previous studies suggesting that CPP-mediated delivery of Cas9 is inefficient[15,16], and that the identity and configuration of CPP and NLS might not be the only key factors limiting efficiency.

We next considered the possibility of potentiating cell penetration and endosomal escape through the action of assist chemicals or assist peptides (APs) acting in *trans* with Cas-CPPs (Fig. 1b). To explore this possibility, we co-incubated 0.5 μM Cas9-T6N and mChe reporter cells with a series of assist chemicals and APs with known functions in facilitating cell penetration and/or endosomal escape[17,19] (Fig. 1b). Whereas assist chemicals had minimal effects, we observed promising results with specific configurations of APs (Fig. 1c and Supplementary Fig. 2). TAT-HA2 is a fusion peptide consisting of a CPP derived from HIV trans-activator of transcription (TAT) protein[20] and an endosomal escape AP from influenza A virus hemagglutinin (HA2) protein[21]. Remarkably, the TAT-HA2 fusion, but neither TAT nor HA2 alone, potentiated Cas9-T6N editing of the mChe reporter from an undetectable level to up to ~85% efficiency (Fig. 1c). Furthermore, TAT-HA2 enabled gene editing at a tenfold lower concentration of Cas9-T6N protein with minimal loss of editing efficiency (Supplementary Fig. 5a) and minimum cellular toxicity (Fig. 1e and Supplementary Fig. 5b). Even at a 100-fold lower concentration (0.05 μM) of Cas9-T6N protein, TAT-HA2 editing still occurred in ~40% of cells (Supplementary Fig. 5a).

To explore how TAT-HA2 increased editing efficiency, we monitored cellular uptake and nuclear localization of Cas9-T6N via cell fractionation. The addition of TAT-HA2 increased the cell penetration efficiency of Cas9-T6N by ~5-fold and dramatically increased the nuclear localization of Cas9-T6N by ~62-fold (Fig. 1f). To test whether TAT-HA2 could act in *cis*, we linked the HA2 to Cas9-T6N, generating a TAT-HA2-4xNLS-Cas9-2xNLS-sfGFP (Cas9-TH6N). This modification failed to improve gene editing, suggesting that TAT-HA2 is required in *trans*, rather than in *cis*, to facilitate the gene editing of Cas9-CPPs (Supplementary Fig. 6). Furthermore, TAT-HA2 improved the gene editing efficiency of all six different Cas9-CPPs we had previously tested, regardless of the CPP identity and configuration (Supplementary Fig. 4b). Collectively, the addition of TAT-HA2 enabled increased gene editing efficiency even with substantially decreased amounts of Cas9-CPPs and for multiple different Cas9-CPPs, suggesting that the co-incubation with TAT-HA2 is a crucial factor to release the full potential of Cas9-CPP. We term the combination of a Cas-CPP protein and an assist endosomal escape peptide (AP; here TAT-HA2) as PAGE.

We tested whether the mechanisms that render Cas9-PAGE highly efficient in EL4 cells would apply in other cell types, including primary cells. We inserted the mChe gene editing reporter in a human myeloid cell line, a human natural killer cell line and finally primary human T cells isolated from peripheral blood of three different healthy donors (Fig. 1g). In all cases, Cas9-PAGE demonstrated robust gene editing, approximating 80–90%, in both human cell lines and primary cells (Fig. 1h), which indicates that PAGE is applicable to diverse cell types.

Robust Cas9-PAGE genome editing in clinically relevant models of mouse primary T cells

Given the robust gene editing efficiency of PAGE in reporter cell lines with a single integrated copy of mChe, we next evaluated the performance of PAGE in biallelic editing of endogenous genes in primary mouse $CD8^+$ T cells. To set up the PAGE system for targeting endogenous genes, we first retrovirally transduced the mouse $CD8^+$ T cells with a bicistronic vector expressing either an experimental sgRNA or sgNeg along with an mChe marker. The sgRNA-positive cell population was enriched by sorting mChe-positive cells. We next incubated these cells for 30 min with Cas9-PAGE (Fig. 2a). Notably, monitoring of Cas9-T6N-associated GFP fluorescence indicated that Cas9-PAGE uptake occurred shortly after incubation and diminished to a background level within 3 d (Supplementary Fig. 7). We first tested sgRNAs targeting a nonessential endogenous gene in the T cells, *Thy1*, encoding the cell surface protein CD90. Of note, Cas9-PAGE reduced surface CD90 expression by >90%, indicating that both *Thy1* alleles were targeted (Fig. 2b,c). Efficient editing was dependent on the addition of the AP, consistent with observations using mChe reporter cell lines

(Fig. 2b,c and Supplementary Fig. 8). We further evaluated the gene editing efficiency of Cas9-PAGE with additional independent sgRNAs targeting *Thy1* or another nonessential gene in T cells, *Ptprc* (encoding CD45 protein). Flow cytometry and TIDE indel analysis confirmed that Cas9-PAGE-mediated high efficiency on-target mutagenesis of both genes in mouse primary CD8$^+$ T cells (Supplementary Fig. 9a,b).

CRISPR-based genetic studies of T cells in vivo have been challenging due to the requirement for generating transgenic mice with Cas9 expression in antigen-specific T cells[9–12]. To evaluate the performance of Cas9-PAGE for in vivo studies in CD8$^+$ T cells, we used the well-characterized model of chronic lymphocytic choriomeningitis virus (LCMV) infection using the LCMV clone 13 strain with P14 T cell receptor (TCR) transgenic CD8$^+$ T cells (P14) specific for the LCMV D^bGP_{33-41} epitope[22]. Infection with LCMV clone 13 leads to the accumulation of exhausted CD8$^+$ T cells, providing a model for studying T cell dysfunction as found occurring under the conditions of chronic infections or in cancer[23]. To begin to examine the utility of the Cas9-PAGE system in vivo, we used a cotransfer system with donor P14 cells on two distinct congenic backgrounds (CD45.1 and CD45.1/2) in the same recipient mice on a third congenic background (CD45.2). This cotransfer system offered advantages to distinguish populations of experimental and control cells in vivo and to control for any environmental changes impacting pathogenesis or T cell biology[24]. P14 cells were activated ex vivo and retrovirally transduced with sgRNAs targeting a nonessential control gene (*Thy1*) in one congenic background (CD45.1) or a negative control gene (*Ano9*) in the second congenic background (CD45.1/2). Both sets of P14 cells were then incubated with Cas9-PAGE and selected by sorting for expression of sgRNA and Cas9-PAGE uptake (Fig. 2d). The congenially distinct P14 cells were mixed at a 1:1 ratio and adoptively transferred into recipient mice of the third congenic background (CD45.2) infected with LCMV clone 13 (Fig. 2d). Targeting *Thy1* with Cas9-PAGE led to the loss of CD90 expression in ~80% of P14 cells at day 8 postinfection (Fig. 2e,f and Supplementary Figs. 10 and 11a), suggesting that Cas9-PAGE was highly efficient in ex vivo engineering T cells for subsequent adoptive T cell transfer in vivo studies.

Exhausted CD8$^+$ T cells are characterized by high expression of inhibitory coreceptors such as PD-1, and targeted blockade or disruption of inhibitory receptors such as PD-1 has revolutionized cancer immunotherapy[25,26]. We next used Cas9-PAGE to target *Pdcd1* (encoding PD-1). At day 8 postinfection, whereas ~80% of sgNeg-transduced P14 cells were PD-1$^+$, only 20% of sg*Pdcd1*-transduced P14 cells expressed PD-1 (Fig. 2g,h and Supplementary Fig. 10 and 11b). PD-1 restrains CD8$^+$ T cell proliferation in response to chronic T cell stimulation and knockout of *Pdcd1* increases CD8$^+$ T cell numbers during chronic infection[27]. We found that by day 15 postinfection, *Pdcd1*-edited P14 had a marked selective advantage over sgNeg-transduced P14 in the blood, representing ~99% of the adoptively transferred P14 cells (Fig. 2i and Supplementary Fig. 11c). This numerical advantage of the *Pdcd1*-edited P14 cells continued throughout the infection (Fig. 2i), with sg*Pdcd1*-transduced P14 cells representing >15% of total CD8$^+$ T cells in the blood of these mice (Fig. 2j). Collectively, Cas9-PAGE-mediated *Pdcd1* knockout in primary mouse P14 cells was similar to that previously observed using traditional approaches, including classical genetic knockouts[9,27], thus highlighting the ability of Cas-PAGE to provide a simple and highly efficient genome editing platform for in vivo CD8$^+$ T cell studies.

High-efficient CRISPR-RNP-PAGE genome editing in human CAR T cells

The combination of Cas9-PAGE delivery with viral sgRNAs can enable in vivo T cell genetic studies, for example, via adoptive T cell transfer experiments. Nonetheless, a single-step direct delivery of an RNP complex, consisting of both Cas9 protein and sgRNA in the PAGE format, could provide a fast, simple and more widely applicable method for genome editing. To test the editing efficiency of Cas9-RNP-PAGE, we formed an RNP complex via mixing Cas9-T6N with sgRNA, followed by transient incubation of the RNP complex with AP and activated mouse CD8$^+$ T cells and then evaluated gene editing via flow cytometry (Fig. 3a). Under the most optimized condition, Cas9-RNP-PAGE targeting *Thy1* only resulted in a relatively inefficient loss of CD90 expression (<10%; Fig. 3b), in contrast to the >90% editing efficiency of using a combination of viral sgRNA and Cas9-PAGE delivery (Fig. 2b).

We hypothesized that the high negative charge of the added ~100-nt Cas9 sgRNA might impact the cell penetration efficiency of Cas9-RNP-PAGE, thus lowering gene editing. To reduce the overall negative charge of the Cas9-RNP-PAGE, we tested whether adding positively charged peptides to Cas9-T6N could increase editing efficiency. However, this addition resulted in only marginal improvements in gene editing (Fig. 3b). As an alternative solution, we next evaluated the RNP-PAGE using an optimized Cas12a (opCas12a) system, in which the opCas12a protein has similar gene editing efficiency to Cas9 (refs. 28–30). The advantage of this approach is that the CRISPR guide RNA (crRNA) for opCas12a is only 40 nt in length[31], thus substantially reducing the overall negative charge of the complex. Indeed, opCas12a-RNP-PAGE targeting *Thy1* resulted in ~8-fold increased gene editing efficiency compared to Cas9-RNP-PAGE, reaching over 70% editing (Fig. 3b). As with Cas9-PAGE, the robust gene editing efficiency of opCas12a-RNP-PAGE was dependent on AP co-incubation (Fig. 3c). Moreover, we further improved the opCas12a-RNP-PAGE gene editing efficiency from ~75% to ~98% by sorting GFP-positive cells shortly after the PAGE incubation, indicating that successful cell penetration with the opCas12a-RNP-PAGE

Fig. 2 | Development of Cas9-PAGE genome editing in clinically relevant models of mouse primary T cells. a, Schematic workflow of Cas9-PAGE system in mouse CD8$^+$ T cells ex vivo. **b**, Quantification of Cas9-PAGE-mediated gene editing of *Thy1* in mouse CD8$^+$ T cells ex vivo. Activated mouse primary CD8$^+$ T cells were retrovirally transduced with either sgThy1_IG1 or sgNeg co-expressing with an mChe reporter. sgRNA$^+$/mChe$^+$ cells were FACS sorted and incubated with 5 μM Cas9-T6N and various concentrations of AP for 30 min. Flow cytometry analysis of surface CD90 level was performed at 4 d after PAGE incubation (n = 2, biological replicates). **c**, A representative flow cytometry plot of surface CD90 expression level of primary CD8$^+$ T cells transduced with indicated sgRNAs at 6 d after PAGE incubation (5 μM Cas9-T6N and 25 μM AP). **d**, Schematic workflow of Cas9-PAGE in mouse primary CD8$^+$ T cells for in vivo study. Donor CD8$^+$ T cells from P14 transgenic (CD45.1$^+$ or CD45.1/2$^+$ congenic) mice were isolated and activated with anti-CD3, anti-CD28 and IL-2, followed by retroviral transduction with either experimental or negative control sgRNA expression vector linked with a fluorescence marker. sgRNA-transduced T cells were incubated with 5 μM Cas9-T6N and 25 μM AP for 30 min before FACS sorting to enrich the Cas9 and sgRNA double positive population. Experimental and negative control sgRNA-transduced P14 T cells were mixed in a 1:1 ratio, followed by adoptive transfer to CD45.2$^+$ congenic recipient mice that were infected with LCMV clone13 virus. Gene editing and P14 T cell population were evaluated by flow cytometry over a time course of 30 d. **e**,**f**, Example flow cytometry plot (**e**) and quantification of CD90 surface expression (**f**) following Cas9-PAGE-mediated editing at day 8 postinfection (n = 10, biological replicates). sgThy1_IG1 was designed to target the immunoglobulin-like domain (IG) of *Thy1*. **g**,**h**, Example flow cytometry plot (**g**) and quantification of PD-1 surface expression (**h**) following Cas9-PAGE-mediated editing at day 8 postinfection (n = 9, biological replicates). sgPdcd1_IG44 was designed to target the IG of *Pdcd1*. CD44$^+$ CD8$^+$ T cells were used as a positive control for CD90 expression in flow cytometry plot (**e**). Lack of CD44 expression (CD44$^-$) was used to identify naive CD8$^+$ T cells as a negative control for PD-1 expression in flow cytometry plot (**g**). **i**, Proportion of cotransferred P14 T cells transduced with indicated sgRNA in blood over time. P14, CD8$^+$ T cells with specific T cell receptor for the LCMV D^bGP_{33-41} epitope. **j**, P14 T cells transduced with indicated sgRNAs as a proportion of total CD8$^+$ T cells in blood over a time course of 30 d. n = 10 in the days 8 and 15 postinfection samples, n = 5 in the days 22 and 30 postinfection samples, biological replicates (**i**,**j**). P values are indicated (two-tailed Wilcoxon matched-pairs signed rank test). Error bars smaller than the symbol width were not shown. Data were presented as mean ± s.e.m.

https://doi.org/10.1038/s41587-023-01756-1

system yields optimal genome editing efficiency (Fig. 3d). Thus, opCas12a-RNP-PAGE provides a simple and robust gene editing method for mouse primary T cells.

Genome engineering of CAR T cells holds great promise to improve therapeutic efficacy[4]. We wanted to test whether the opCas12a-RNP-PAGE system could be incorporated into a standard

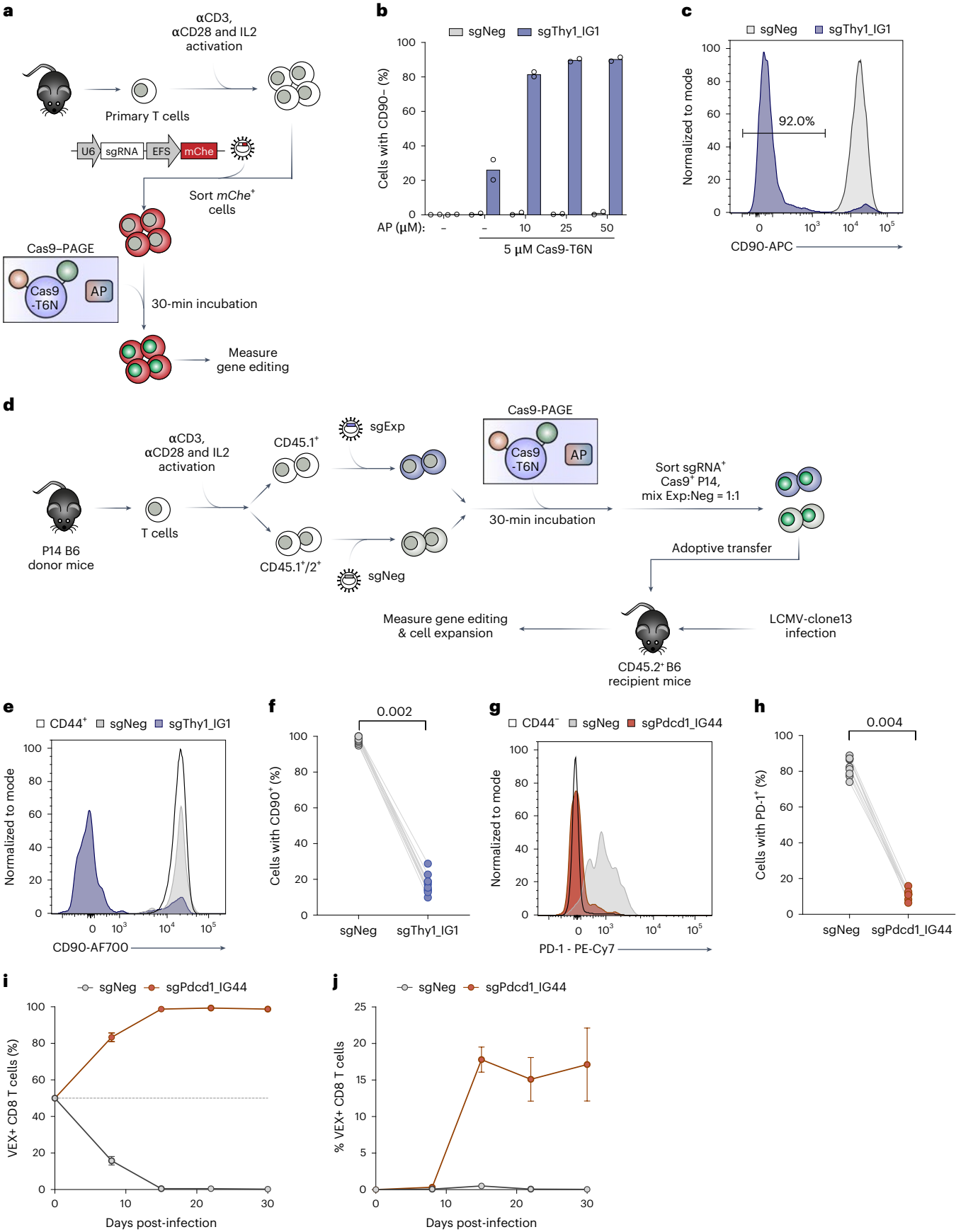

CAR T cell production process and whether this approach could overcome some of the limitations of electroporation-based approaches (Fig. 3e). Therefore, we compared CD19-specific CAR T cells (CAR19) that had been incubated transiently with opCas12a-RNP-PAGE loaded with a nontargeting negative control crRNA to CAR19 that had been treated with conventional electroporation method (Fig. 3e). We found that opCas12a-RNP-PAGE had minimal cellular toxicity and resulted in approximately 98% recovery of live CAR19 cells postincubation, compared to approximately 68% recovery from electroporation treatment (Fig. 3f). The opCas12a-RNP-PAGE edited CAR19 cells also showed efficient ex vivo expansion over 10 d, similar to unedited control cells, outperforming the electroporation treated cells (Fig. 3g and Supplementary Fig. 12). To evaluate the impact of the treatments on global transcriptional changes, we performed RNA-seq analysis on CAR19 cells at 6 h and 3 d post-treatment with either opCas12a-RNP-PAGE or electroporation. Principal component analysis of the RNA-seq data revealed high similarity between the opCas12a-RNP-PAGE-edited and mock control CAR19 cells that clustered closely together in principal component space and separated from the electroporated cells, especially in the first principal component at both time points post-treatment (Fig. 3h and Supplementary Fig. 13a). Notably, compared to the mock control, opCas12a-RNP-PAGE-edited CAR19 cells showed no significant gene expression changes at a threshold of absolute $\log_2$(fold change) > 0.5 and adjusted $P < 0.01$. This lack of transcriptional changes in the opCas12a-RNP-PAGE-edited CAR19 cells contrasted with the electroporated CAR19 cells that displayed 1,986 and 421 gene expression changes at 6 h and 3 d post-treatment, respectively (Fig. 3i and Supplementary Fig. 13b). Additionally, in a coculture killing assay with CAR19 and tumor cells, there were no differences in cytotoxicity between opCas12a-RNP-PAGE-edited CAR19 cells and untreated control cells (Supplementary Fig. 14). Collectively, these results suggest that the opCas12a-RNP-PAGE system can permit delivery of editing machinery without a negative impact on cell growth, anti-tumor function or transcriptional programs of CAR T cells.

Then, to evaluate the gene editing efficiency in CAR19 cells, we loaded the opCas12a-RNP-PAGE with crRNAs targeting either the nonessential genes, *PTPRC, B2M*, or *TRAC*. *B2M* and *TRAC* are currently being targeted for next-generation CAR T cells as part of allogeneic cell therapy approaches[32] and for the improvement of CAR T cell functionality[33]. Consistent with the results obtained above in mouse primary T cells, we found that opCas12a-RNP-PAGE-mediated gene editing of *PTPRC* in CAR19 cells was dependent on AP co-incubation and resulted in minimal cellular toxicity with normal ex vivo expansion capacity (Fig. 3j,k and Supplementary Fig. 15). The opCas12a-RNP-PAGE approach resulted in ~30% to 70% gene editing of *PTPRC*, ~95% gene editing of *B2M* and ~75% gene editing of *TRAC* as determined by flow cytometric analysis of protein expression (Fig. 3j,l and Supplementary Figs. 16 and 17). On-target genome editing was further confirmed with TIDE indel analysis (Supplementary Fig. 18). Although the Cas9-RNP-PAGE system initially showed lower gene editing efficiency in mouse primary T cells, we also examined ways to improve the performance of this system in CAR T cells. To start, we performed Cas9-RNP-PAGE in CAR19 cells using a single sgRNA. By analyzing deep sequencing data of the sgRNA on-target and well-established sgRNA-dependent off-target sites, we found that the gene editing efficiency of Cas9-RNP-PAGE in CAR19 cells was relatively low, consistent with the data from primary mouse T cells above. Nonetheless, Cas9-RNP-PAGE maintained a high on-target versus off-target editing ratio, indicating that the method of PAGE delivery did not have a significant effect on off-target editing (Supplementary Fig. 19). To improve the gene editing efficiency of Cas9-RNP-PAGE in CAR19 T cells, we optimized the PAGE protocol and found a combination of RNP complex formation conditions, using pooled sgRNAs instead of single sgRNA, and increased AP concentration (Methods) substantially improved the knockout efficiency of

Fig. 3 | Development of CRISPR-RNP-PAGE genome editing in human CAR T cells. a, A schematic workflow of Cas RNP complex of PAGE in mouse primary CD8$^+$ T cells ex vivo. Cas9-T6N, Cas9-T8N or opCas12a-T8N was mixed with its associated guide RNA to form an RNP complex before co-incubation with activated mouse primary CD8$^+$ T cells. **b**, Quantification of Cas9-T6N-RNP, Cas9-T8N-RNP or opCas12a-T8N-RNP-mediated gene editing of *Thy1* in mouse CD8$^+$ T cells ex vivo. Cells were incubated with either 5 μM Cas9-T6N-RNP, Cas9-T8N-RNP or opCas12a-T8N-RNP and 25 μM AP for 30 min. Flow cytometry analysis of surface CD90 level was performed at 5 d after RNP-PAGE incubation ($n = 2$, biological experiments from two donor mice). **c**, Quantification of opCas12-RNP-PAGE-mediated gene editing of *Thy1* in mouse CD8$^+$ T cells with various concentrations of AP ex vivo. Cells were incubated with 5 μM opCas12a-T8N-RNP and indicated concentrations of AP for 30 min. Flow cytometry analysis of surface CD90 level was performed at 5 d after opCas12-RNP-PAGE incubation ($n = 3$, biological experiments from three different donor mice). **d**, Representative flow cytometry plot of surface CD90 expression level of primary CD8$^+$ T cells treated with opCas12-RNP-PAGE. Cells were either sorted or not based on the GFP positivity right after the incubation with 5 μM opCas12-T8N-RNP and 25 μM AP, followed by flow cytometry analysis of surface CD90 level at 5 d after PAGE incubation. sgThy1_IG1 and crThy1_IG1 were designed to target the IG of *Thy1*. Error bars smaller than the symbol width were not shown. Data were presented as mean ± s.d. **e**, Schematic workflow of either RNP-PAGE or RNP electroporation in human CAR19 cells ex vivo. CAR19, a CAR of T cells, specifically recognizes the CD19 antigen. Human primary T cells from healthy donors were isolated and activated with anti-CD3, anti-CD28 and IL-2. Activated T cells were transduced with CAR19 lentivirus 1-d post-activation. On day 4 postinfection, CAR19$^+$ cells were FACS sorted before treatment with either opCas12a-RNP-PAGE or opCas12a-RNP electroporation. **f**, Live cells were quantified 6-h post-treatment with either opCas12a-RNP-PAGE or electroporation. The data were normalized to the mock treatment control group ($n = 6$, representing biological replicates from three health donors). **g**, Expansions of PAGE-treated or electroporated CAR19 cells were monitored over a time course of 10 d. **h**, A principal component analysis plot of RNA-seq data for CAR19 cells at 6-h post-treatment of either PAGE or electroporation is shown, with $n = 4$ representing biological replicates from two healthy donors. **i**, MA plot of the $\log_2$ fold change of all genes in either PAGE-treated or electroporated CAR19 cells from **h**. The differential gene expression statistical test was performed using DESeq2, which employs a default two-sided Wald test with Benjamini–Hochberg multiple test correction. The *x*-axis represents the mean of the read counts of replicates, while the *y*-axis shows the $\log_2$ fold change calculated by DESeq2 with batch correction. Blue dots indicate genes with a Benjamini–Hochberg adjusted $P < 0.01$ and an absolute $\log_2$ fold change greater than 0.5. Blue dotted lines indicate an absolute $\log_2$fold change of 0.5. **j**, Quantification of opCas12a-T8N-RNP-mediated gene editing of *PTPRC* in CAR19 ex vivo. Cells were incubated with 5 μM opCas12a-T8N-RNP with or without 25 μM AP for 30 min. Cell surface CD45 expression level was measured via flow cytometry analysis at 6 d after RNP-PAGE incubation ($n = 2$, biological replicates). crRNAs were designed to target the catalytic domain (CAT) of *PTPRC*. **k**, Live cells were quantified immediately following either mock or opCas12a-RNP-PAGE incubation. The data were normalized to the mock treatment control group ($n = 4$, biological replicates representing four health donors). **l**, Quantification of opCas12a-RNP-PAGE-mediated gene editing of *B2M* in CAR19 ex vivo. Cell surface B2M level was measured via flow cytometry at 10 d after RNP-PAGE incubation ($n = 2$, representing biological replicates from two health donors). crRNAs were designed to target the IG of *B2M*. **m**,**n**, Quantification of Cas9-RNP-PAGE-mediated gene editing of *B2M* in CAR19 cells ex vivo. Cells were incubated with 5 μM of Cas9-T6N under indicated conditions of AP and sgRNA for 30 min. Flow cytometry analysis of surface B2M level was performed 10 d after Cas9-RNP-PAGE incubation ($n = 2$ in the 25 μM AP group in (m), $n = 3$ in the 75 μM AP group in **m** and $n = 2$ in **n**, representing biological experiments from two health donors). **o**, Representative flow cytometry plot of surface B2M expression level of CAR19 cells treated with Cas9-RNP-PAGE. Cells were either sorted or not based on the GFP positivity right after the incubation with 5 μM Cas9-T6N-RNP and 75 μM AP, followed by flow cytometry analysis of surface B2M level at 10 d after PAGE incubation. **p**, Live cells were quantified immediately following either mock or Cas9-RNP-PAGE incubation. The data were normalized to the mock treatment control group ($n = 2$, representing biological experiments from two health donors). Data were presented as mean ±s.d. ND, normal donor; electro, electroporation.

https://doi.org/10.1038/s41587-023-01756-1

B2M to ~75% (Fig. 3m,n). Additionally, sorting GFP-positive cells further improved gene editing efficiency, reaching ~87% (Fig. 3o). These CAR19 T cells, edited by Cas9-RNP-PAGE with increased AP and pooled sgRNAs, underwent efficient ex vivo expansion over 10 d, similar to unedited control cells, with minimal cell death associated with PAGE treatment (Fig. 3p and Supplementary Fig. 20). Collectively, these

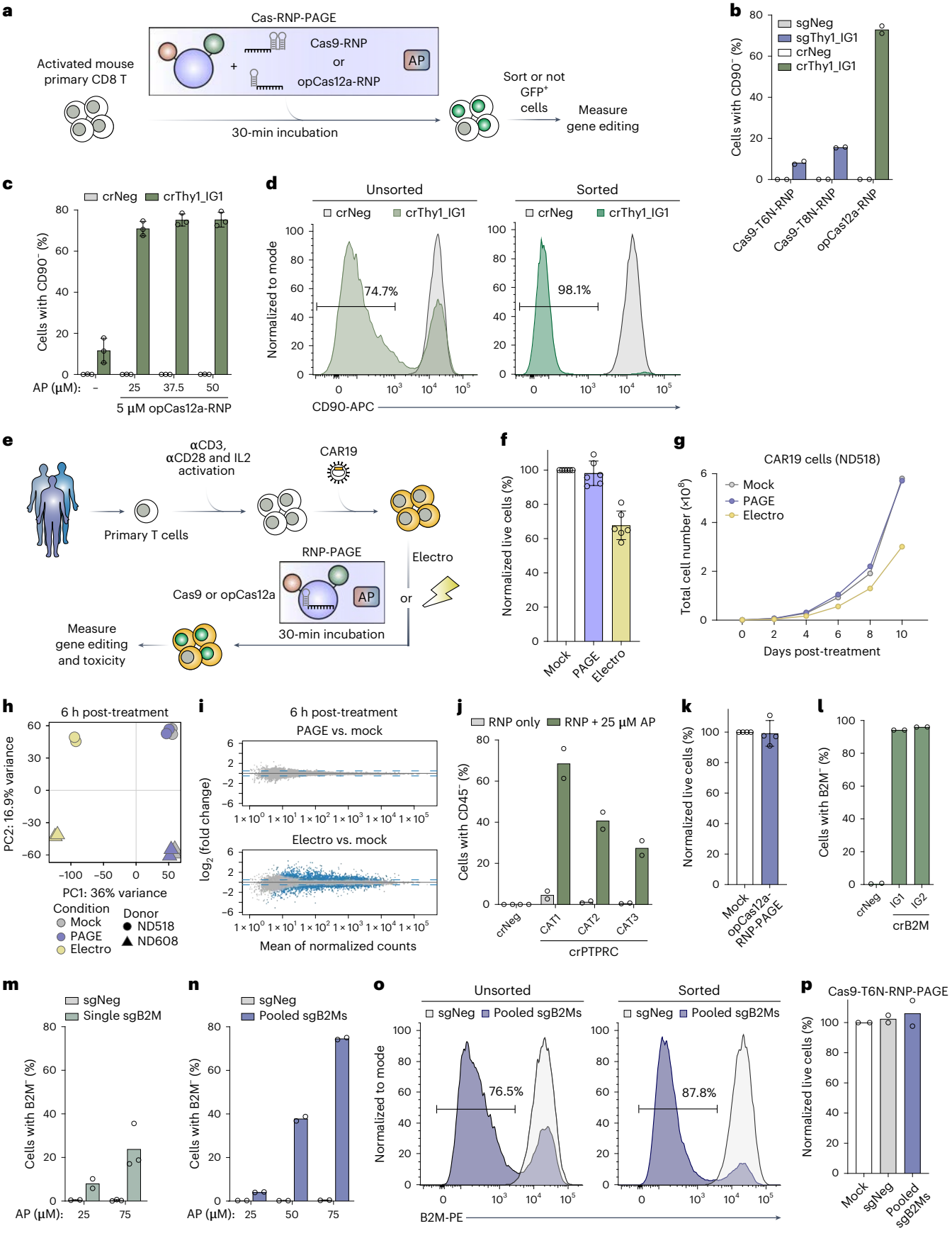

https://doi.org/10.1038/s41587-023-01756-1

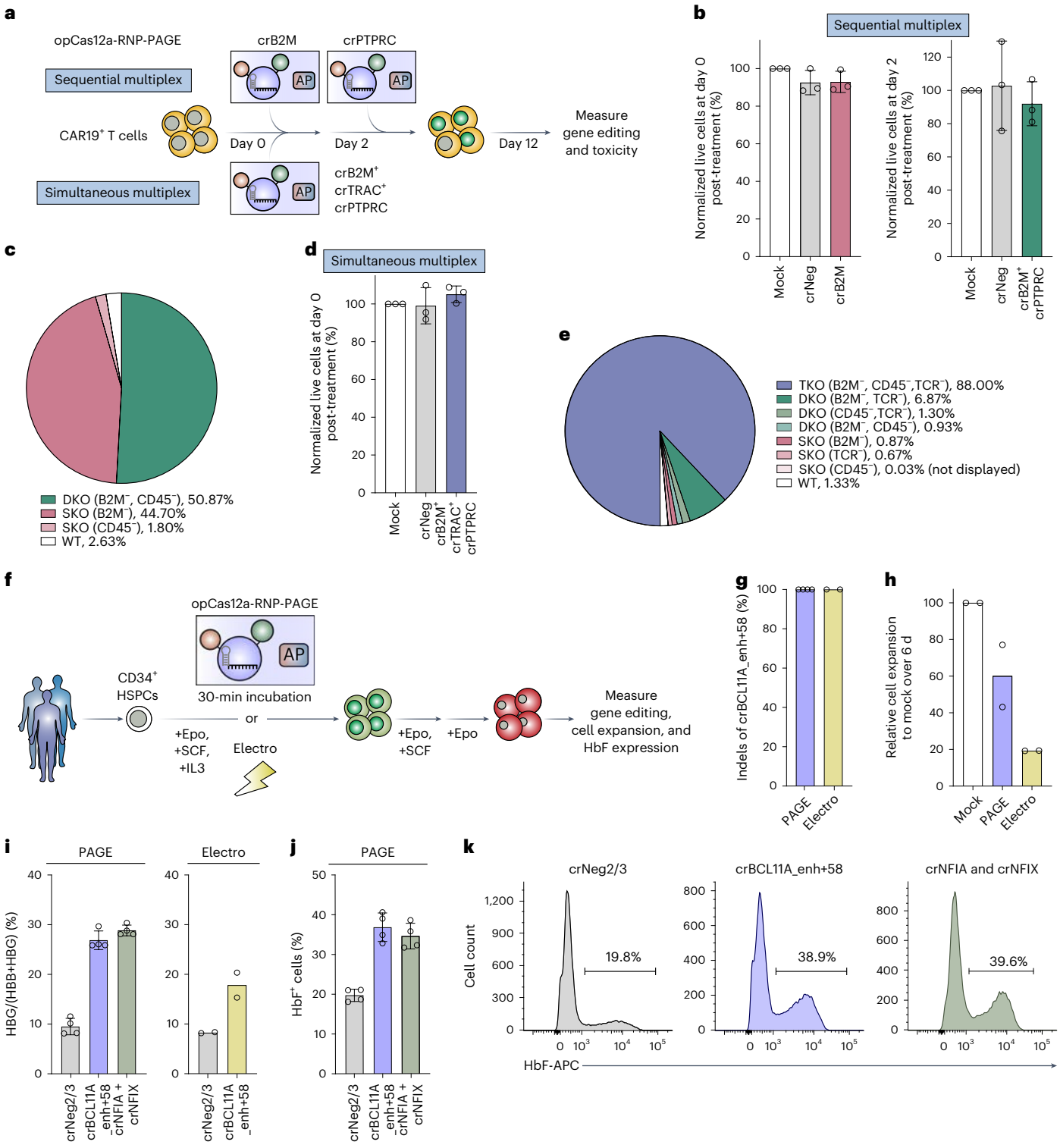

data demonstrate the simplicity and high efficiency of Cas-RNP-PAGE in genome engineering of primary mouse and human T cells with minimal toxicity.

PAGE-mediated robust multiplex genome editing in human CAR T cells and HSPCs

Multiplex genome editing is necessary to engineer next-generation CAR T cells for optimal therapeutic efficacy[6,32]. We aimed to evaluate the potential of Cas-RNP-PAGE for multiplex gene editing in CAR T cells, focusing on the use of the opCas12a-RNP-PAGE system due to its relative simplicity and high efficiency. The minimal cellular toxicity associated with the Cas-RNP-PAGE system offers the opportunity to conduct either sequential or concurrent multiplex genome editing. To test this idea, we first performed a sequential double knockout of *B2M* and *PTPRC* in CAR19 cells by transient incubation with opCas12a-RNP-PAGE targeting *B2M* at day 0, followed by a second incubation with opCas12a-RNP-PAGE targeting *PTPRC* after 2 d (Fig. 4a). As expected, minimal cell toxicity was observed at both time points with sequential opCas12a-RNP-PAGE editing in CAR19 cells (Fig. 4b). The opCas12a-RNP-PAGE-mediated sequential gene editing of *B2M* and *PTPRC* resulted in ~50.9% of the

Fig. 4 | PAGE-mediated multiplex genome editing in human CAR T cells and HSPCs. a, Schematic workflow of opCas12-RNP-PAGE-mediated multiplex gene editing in human CAR19 ex vivo. The sequential double knockout of *B2M* and *PTPRC* was performed by incubating CAR19 cells with opCas12a-RNP-PAGE containing a single crRNA targeting *B2M* on day 0 for 30 min, followed by a second 30-min incubation with opCas12a-RNP-PAGE containing a single crRNA targeting *PTPRC* 2 d later. For the simultaneous triple knockout of *B2M*, *TRAC* and *PTPRC*, opCas12a-RNP-PAGE containing a mixture of three crRNA targeting each gene was incubated with CAR19 for 30 min. Cellular toxicity was evaluated immediately after each PAGE incubation, and gene editing efficiency was measured 10 d after PAGE treatment. **b**,**d**, Live cells were quantified immediately following either mock or opCas12a-RNP-PAGE incubation. The data were normalized to the mock treatment control group ($n = 3$, representing biological experiments from three health donors). **c**,**e**, Quantification of opCas12a-RNP-PAGE-mediated multiplex gene editing in CAR19 ex vivo. Cell surface B2M and CD45 levels were measured via flow cytometry at 10 d after RNP-PAGE incubation in the sequential multiplex gene editing (**c**). Cell surface B2M, CD45 and TCR levels were measured via flow cytometry at 10 d after RNP-PAGE incubation in the simultaneous multiplex gene editing (**e**) ($n = 3$, representing biological experiments from three health donors). **f**, Schematic workflow of ex vivo genome engineering of primary human HSPCs using either opCas12a-RNP-PAGE or Cas12a-RNP electroporation methods. HSPCs were obtained from healthy donors and treated with either PAGE or electroporation methods. The HSPCs were then differentiated into erythroid cells using a three-phase erythroid differentiation protocol, followed by assessment of genome editing efficiency, cell expansion and reactivation of fetal hemoglobin. **g**, Quantification of gene editing efficiency of *BCL11A* + 58 kb enhancer using either PAGE or electroporation. The bar graph depicts the TIDE assay score (indel%), on-target mutagenesis efficiency, of indicated method ($n = 4$ in the PAGE treatment group and $n = 2$ in the electroporation treatment group, representing biological replicates from two different health donors). **h**, Relative cell expansion of $CD34^+$ HSPCs edited by either PAGE or electroporation methods. The number of live cells was quantified at day 6 after gene editing using either PAGE or electroporation methods. The data were normalized to the mock treatment control group ($n = 2$, representing biological experiments from two health donors). **i**, qRT-PCR analysis of fetal globin transcripts (HBG) of total globin transcripts (HBG + HBB) on day 13 after gene editing using either opCas12a-RNP-PAGE or Cas12a-RNP electroporation. HBG, hemoglobin subunit gamma 1 and 2, HBB, hemoglobin subunit beta. Negative control crRNA, crNeg2/3, targeting *GCG* and non-expressed genes in HSPCs were used ($n = 4$ in the PAGE treatment group and $n = 2$ in the electroporation treatment group, representing biological replicates from two different health donors). **j**, Summary of HbF flow cytometry of primary erythroid precursor cells edited by opCas12a-RNP-PAGE with indicated crRNAs ($n = 4$, representing biological replicates from two health donors). **k**, Representative flow cytometry plot of intracellular HbF staining from **j**. Data were presented as mean ± s.d. Electro, electroporation.

CAR19 cell population losing both cell surface proteins, as well as ~44.7% and ~1.8% of the population losing either B2M or PTPRC alone, respectively (Fig. 4c and Supplementary Fig. 21). The preferential loss of B2M compared to PTPRC was likely due to the sequential order of gene editing. To further test the multiplex capacity of opCas12a-RNP-PAGE, we performed a simultaneous triple knockout of *B2M*, *TRAC* and *PTPRC* in CAR19 cells by opCas12a with mixing pooled crRNAs targeting these three genes (Fig. 4a). This opCas12a-RNP-PAGE-mediated triple knockout was well-tolerated in CAR19 cells with minimal cell toxicity (Fig. 4d). Remarkably, transient exposure to the opCas12a-RNP-PAGE resulted in ~88.0% of the CAR19 cell population losing cellular surface staining of CD45, B2M and TCR, with a smaller fraction of doubly or singly edited cells and only about 1.3% of the population being unedited (Fig. 4e and Supplementary Fig. 22). Collectively, these data demonstrate the high efficiency of Cas-RNP-PAGE for multiplex editing of primary T cells and define this approach as a facile tool for ex vivo engineering of next-generation CAR T cells with minimal toxicity.

To assess the broader potential of the opCas12a-RNP-PAGE system beyond gene editing in primary T cells, we aimed to genome engineer human $CD34^+$ hematopoietic stem and progenitor cells (HSPCs). HSPCs can differentiate into various hematopoietic lineages, and genome editing in HSPCs may enable gene therapies for hematologic diseases[34]. Here we differentiated HSPCs toward the erythroid lineage following opCas12a-RNP-PAGE editing of the hematopoietic progenitors (Fig. 4f) using a three-phase erythroid differentiation protocol[35]. We chose the *BCL11A* gene as a target. BCL11A is a transcription factor that represses fetal hemoglobin (HbF) gene expression in erythroid cells. Conventional genome editing to modulate *BCL11A* expression via targeting its erythroid-specific intronic enhancer (+58 kb) is being investigated clinically for the treatment of sickle cell disease and some forms of β-thalassemia.[36,37] For comparison, the same *BCL11A* +58 kb enhancer was targeted in HSPCs-derived progenitors using both transient opCas12a-RNP-PAGE treatment and conventional electroporation method. The efficiency of genome editing, cell expansion and activation of HbF in HSPC-derived erythroid cells was then evaluated (Fig. 4f). Both RNP-PAGE and RNP electroporation resulted in ~100% editing of the *BCL11A* +58 kb enhancer as measured by TIDE indel analysis (Fig. 4g). PAGE-edited HSPCs generated approximately three times more erythroid cells compared to electroporated cells after 6 d of expansion, suggesting that the PAGE editing is less detrimental to cell viability than electroporation (Fig. 4h). qRT-PCR analysis confirmed an increased proportion of fetal globin transcripts of total globin transcripts (Fig. 4i). Flow cytometry further showed that opCas12a-RNP-PAGE edited cells gave rise to an increased proportion of HbF^+ cells with therapeutically relevant levels of HbF production (Fig. 4j,k). In addition, we further validated the multiplexing capabilities of the opCas12a-RNP-PAGE system in HSPCs-derived progenitors by performing a double knockout of *NFIA* and *NFIX*, two recently identified fetal HbF silencers[38]. Accordingly, PAGE-mediated double knockout of *NFIA*- and *NFIX*-activated HbF reactivation at both mRNA and protein levels, as measured by qRT-PCR and flow cytometry (Fig. 4i–k). Together, these data support the use of opCas12a-RNP-PAGE as a simple and robust approach for ex vivo hematopoietic progenitor cell gene editing and provide a strong rationale for generalizing the CRISPR-PAGE platform for genome engineering of primary hematopoietic lineage cells.

Discussion

Our results demonstrate that CRISPR-PAGE offers a rapid and facile genome editing system with high efficiency (Supplementary Fig. 1). Using 30-min transient incubation, both Cas-PAGE and Cas-RNP-PAGE result in up to ~98% editing efficiency in mouse and human primary T cells, as well as close to ~100% gene editing efficiency in HSPCs. We demonstrate that PAGE offers a broadly adaptable platform that is easy to implement for in vivo genetic studies using mouse T cells in disease models, for ex vivo engineered adoptive T cell therapies using human cells and for gene therapy using human hematopoietic progenitor cells. The potential for pre-existing immunity against components of the PAGE system may limit its use for in vivo delivery but is relatively less of a concern for ex vivo gene editing. Further research is needed to fully evaluate the immunogenicity of the CRISPR-PAGE system in primary cells. Relative to genetic-delivery systems, such as viral-, DNA- and RNA-based methods, transient protein-based editing with PAGE offers multiple potential benefits—reduced risk of off-target editing, decreased Cas immunogenicity, avoidance of potential risks and complications of viral integration, and bypassing deleterious effects on cell viability and/or activation state associated with electroporation. The simplicity of modifications required suggests that, beyond Cas9 and Cas12a, PAGE could facilitate cellular delivery of other genome editing proteins, such as orthogonal Cas proteins, Cas-derived Base Editors, Prime Editors, and Cas integrase[39–45]. PAGE can also be readily re-engineered and expanded for other macromolecules and protein-based therapeutic

delivery. Collectively, PAGE provides a generalizable platform for the delivery of genome editing proteins in a rapid and highly efficient manner to help fostering the next wave of genome engineering focused on primary cells.

Online content

Any methods, additional references, Nature Portfolio reporting summaries, source data, extended data, supplementary information, acknowledgements, peer review information, details of author contributions and competing interests, and statements of data and code availability are available at https://doi.org/10.1038/s41587-023-01756-1.

References

1. Doudna, J. A. The promise and challenge of therapeutic genome editing. *Nature* **578**, 229–236 (2020).
2. Hsu, P. D., Lander, E. S. & Zhang, F. Development and applications of CRISPR–Cas9 for genome engineering. *Cell* **157**, 1262–1278 (2014).
3. Komor, A. C., Badran, A. H. & Liu, D. R. CRISPR-based technologies for the manipulation of eukaryotic genomes. *Cell* **168**, 20–36 (2017).
4. June, C. H., O'Connor, R. S., Kawalekar, O. U., Ghassemi, S. & Milone, M. C. CAR T cell immunotherapy for human cancer. *Science* **359**, 1361–1365 (2018).
5. Rosenberg, S. A., Restifo, N. P., Yang, J. C., Morgan, R. A. & Dudley, M. E. Adoptive cell transfer: a clinical path to effective cancer immunotherapy. *Nat. Rev. Cancer* **8**, 299–308 (2008).
6. Stadtmauer, E. A. et al. CRISPR-engineered T cells in patients with refractory cancer. *Science* **367**, eaba7365 (2020).
7. Atsavapranee, E. S., Billingsley, M. M. & Mitchell, M. J. Delivery technologies for T cell gene editing: applications in cancer immunotherapy. *EBioMedicine* **67**, 103354 (2021).
8. Yin, H., Kauffman, K. J. & Anderson, D. G. Delivery technologies for genome editing. *Nat. Rev. Drug Discov.* **16**, 387–399 (2017).
9. Chen, Z. et al. In vivo $CD8^+$ T cell CRISPR screening reveals control by Fli1 in infection and cancer. *Cell* **184**, 1262–1280 (2021).
10. Dong, M. B. et al. Systematic immunotherapy target discovery using genome-scale in vivo CRISPR screens in CD8 T cells. *Cell* **178**, 1189–1204 (2019).
11. Wei, J. et al. Targeting REGNASE-1 programs long-lived effector T cells for cancer therapy. *Nature* **576**, 471–476 (2019).
12. Huang, H. et al. In vivo CRISPR screening reveals nutrient signaling processes underpinning $CD8^+$ T-cell fate decisions. *Cell* **184**, 1245–1261 (2021).
13. LaFleur, M. W. et al. A CRISPR–Cas9 delivery system for in vivo screening of genes in the immune system. *Nat. Commun.* **10**, 1668 (2019).
14. Zuris, J. A. et al. Cationic lipid-mediated delivery of proteins enables efficient protein-based genome editing in vitro and in vivo. *Nat. Biotechnol.* **33**, 73–80 (2015).
15. Ramakrishna, S. et al. Gene disruption by cell-penetrating peptide-mediated delivery of Cas9 protein and guide RNA. *Genome Res.* **24**, 1020–1027 (2014).
16. Staahl, B. T. et al. Efficient genome editing in the mouse brain by local delivery of engineered Cas9 ribonucleoprotein complexes. *Nat. Biotechnol.* **35**, 431–434 (2017).
17. Erazo-Oliveras, A., Muthukrishnan, N., Baker, R., Wang, T. Y. & Pellois, J. P. Improving the endosomal escape of cell-penetrating peptides and their cargos: strategies and challenges. *Pharmaceuticals (Basel)* **5**, 1177–1209 (2012).
18. Heitz, F., Morris, M. C. & Divita, G. Twenty years of cell-penetrating peptides: from molecular mechanisms to therapeutics. *Br. J. Pharmacol.* **157**, 195–206 (2009).
19. Varkouhi, A. K., Scholte, M., Storm, G. & Haisma, H. J. Endosomal escape pathways for delivery of biologicals. *J. Control. Release* **151**, 220–228 (2011).
20. Frankel, A. D. & Pabo, C. O. Cellular uptake of the tat protein from human immunodeficiency virus. *Cell* **55**, 1189–1193 (1988).
21. Wadia, J. S., Stan, R. V. & Dowdy, S. F. Transducible TAT-HA fusogenic peptide enhances escape of TAT-fusion proteins after lipid raft macropinocytosis. *Nat. Med.* **10**, 310–315 (2004).
22. Wherry, E. J. T cell exhaustion. *Nat. Immunol.* **12**, 492–499 (2011).
23. Wherry, E. J. & Kurachi, M. Molecular and cellular insights into T cell exhaustion. *Nat. Rev. Immunol.* **15**, 486–499 (2015).
24. Kurachi, M. et al. Optimized retroviral transduction of mouse T cells for *in vivo* assessment of gene function. *Nat. Protoc.* **12**, 1980–1998 (2017).
25. Barber, D. L. et al. Restoring function in exhausted CD8 T cells during chronic viral infection. *Nature* **439**, 682–687 (2006).
26. Sharma, P. & Allison, J. P. The future of immune checkpoint therapy. *Science* **348**, 56–61 (2015).
27. Odorizzi, P. M., Pauken, K. E., Paley, M. A., Sharpe, A. & Wherry, E. J. Genetic absence of PD-1 promotes accumulation of terminally differentiated exhausted $CD8^+$ T cells. *J. Exp. Med.* **212**, 1125–1137 (2015).
28. Gier, R. A. et al. High-performance CRISPR–Cas12a genome editing for combinatorial genetic screening. *Nat. Commun.* **11**, 3455 (2020).
29. Kleinstiver, B. P. et al. Engineered CRISPR–Cas12a variants with increased activities and improved targeting ranges for gene, epigenetic and base editing. *Nat. Biotechnol.* **37**, 276–282 (2019).
30. DeWeirdt, P. C. et al. Optimization of AsCas12a for combinatorial genetic screens in human cells. *Nat. Biotechnol.* **39**, 94–104 (2021).
31. Zetsche, B. et al. Cpf1 is a single RNA-guided endonuclease of a class 2 CRISPR–Cas system. *Cell* **163**, 759–771 (2015).
32. Ren, J. et al. Multiplex genome editing to generate universal CAR T cells resistant to PD1 inhibition. *Clin. Cancer Res.* **23**, 2255–2266 (2017).
33. Eyquem, J. et al. Targeting a CAR to the TRAC locus with CRISPR/Cas9 enhances tumour rejection. *Nature* **543**, 113–117 (2017).
34. Weissman, I. L. & Shizuru, J. A. The origins of the identification and isolation of hematopoietic stem cells, and their capability to induce donor-specific transplantation tolerance and treat autoimmune diseases. *Blood* **112**, 3543–3553 (2008).
35. Grevet, J. D. et al. Domain-focused CRISPR screen identifies HRI as a fetal hemoglobin regulator in human erythroid cells. *Science* **361**, 285–290 (2018).
36. Frangoul, H. et al. CRISPR-Cas9 gene editing for sickle cell disease and beta-thalassemia. *N. Engl. J. Med.* **384**, 252–260 (2021).
37. Bauer, D. E. et al. An erythroid enhancer of BCL11A subject to genetic variation determines fetal hemoglobin level. *Science* **342**, 253–257 (2013).
38. Qin, K. et al. Dual function NFI factors control fetal hemoglobin silencing in adult erythroid cells. *Nat. Genet.* **54**, 874–884 (2022).
39. Shmakov, S. et al. Diversity and evolution of class 2 CRISPR-Cas systems. *Nat. Rev. Microbiol.* **15**, 169–182 (2017).
40. Rees, H. A. & Liu, D. R. Base editing: precision chemistry on the genome and transcriptome of living cells. *Nat. Rev. Genet.* **19**, 770–788 (2018).
41. Anzalone, A. V. et al. Search-and-replace genome editing without double-strand breaks or donor DNA. *Nature* **576**, 149–157 (2019).
42. Strecker, J. et al. RNA-guided DNA insertion with CRISPR-associated transposases. *Science* **365**, 48–53 (2019).
43. Yarnall, M. T. N. et al. Drag-and-drop genome insertion of large sequences without double-strand DNA cleavage using CRISPR-directed integrases. *Nat. Biotechnol.* (in press).

44. Tou, C. J., Orr, B. & Kleinstiver, B. P. Precise cut-and-paste DNA insertion using engineered type V-K CRISPR-associated transposases. *Nat. Biotechnol.* (in press).
45. Durrant, M. G. et al. Systematic discovery of recombinases for efficient integration of large DNA sequences into the human genome. *Nat. Biotechnol.* (in press).

Publisher's note Springer Nature remains neutral with regard to jurisdictional claims in published maps and institutional affiliations.

Springer Nature or its licensor (e.g. a society or other partner) holds exclusive rights to this article under a publishing agreement with the author(s) or other rightsholder(s); author self-archiving of the accepted manuscript version of this article is solely governed by the terms of such publishing agreement and applicable law.

© The Author(s), under exclusive licence to Springer Nature America, Inc. 2023

Methods

Cell lines

EL4 (ATCC, TIB-39), HEK293T and PlatE cells were cultured in DMEM (Corning, 10-017-CV), supplemented with 10% FBS (Thermo Fisher Scientific, A3160502) and 1× penicillin–streptomycin (Thermo Fisher Scientific, 15140122). MOLM-13 (DSMZ, ACC-554) cells were cultured in RPMI 1640 (Corning, 10-040-CM), supplemented with 10% FBS and 1× penicillin–streptomycin. NK-92 cells (ATCC, CRL-2407) were cultured in Minimum Essential Medium Alpha (Thermo Fisher Scientific, 12000014) supplemented with 1.5 g l^{-1} sodium bicarbonate (Sigma, S5761), 0.2 mM myo-inositol (Sigma, I7508), 0.02 mM folic acid (Sigma, F8758), 12.5% horse serum (Thermo Fisher Scientific, 16050122), 12.5% FBS, 0.1 mM 2-mercaptoethanol (Thermo Fisher Scientific, 21985023) and 200 U ml^{-1} recombinant human IL-2 (rhIL2; Peprotech, 200-02). NALM6 cells expressing GFP were cultured in RPMI 1640 (Corning, 10-040-CM) supplemented with 10% FBS, 1× penicillin–streptomycin, 10 mM HEPES (Thermo Fisher Scientific, 15620080) and 1× nonessential amino acids (NEAA; Thermo Fisher Scientific, 11140050). All cells were cultured at 37 °C with 5% CO_2 and maintained according to the manufacturer's instructions, and cells were tested for mycoplasma and found to be negative by the e-Myco PLUS Mycoplasma PCR Detection Kit (Bulldog Bio, 25234).

Mice

TCR transgenic P14 C57BL/6 mice (TCR specific for LCMV D^bGP_{33-41}) were bred in-house. Recipient C57BL/6 mice of 6–8 weeks old were purchased from NCI. Both male and female mice were used. Mice were housed in a specific-pathogen-free animal facility at the University of Pennsylvania. The ambient room temperature was ~20 °C, and the humidity was ~55%. The light/dark cycle was 12-h on and 12-h off. All mice were used in accordance with the Institutional Animal Care and Use Committee (IACUC) guidelines for the University of Pennsylvania.

LCMV infection

Chronic LCMV titers were determined as previously described[46]. Mice were infected intravenously with 4×10^6 plaque-forming units (PFU) of LCMV clone 13.

Vector construction and sgRNA cloning

To generate the Twinstrep-SUMO-Cas9-6S (Cas9-6S) expression vector for recombinant Cas9 protein expression in bacteria, the protein-coding sequence '4× SV40 NLS-Cas9- 2× SV40 NLS-sfGFP' from 4× NLS-pMJ915v2-sfGFP (Addgene, 88921) was subcloned into Twinstrep-SUMO-huLwCas13a (Addgene, 90097). To generate Cas9-6N, 4× Myc NLS from pRG232 (Addgene, 149723) was subcloned into Cas9-6S to replace the N-terminus 4× SV40. To generate Cas9-8N, 6× Myc NLS from pRG232 (Addgene, 149723) was subcloned into Cas9-6S to replace the N-terminus 4× SV40. To generate Cas9-T6N, Cas9-R6N and Cas9-T8N, PCR mutagenesis with overlapping DNA oligonucleotides complementary to the Cas9-6N or Cas9-8N backbone was used to incorporate the TAT and (Arg) sequences into Cas9-6N or Cas9-8N. To generate Cas9-TH6N, the TAT-HA2 sequence was amplified by PCR and subcloned into the Cas9-6N backbone. To generate opCas12a-T8N, opAsCas12a from pRG232 was subcloned into Cas9-T8N to replace Cas9. The lentiviral LRCherry2.1Tb vector was used to make all the mChe gene editing reporter cell lines in this study. To generate LRCherry2.1Tb, a blasticidin resistance cDNA and P2A coding sequence were PCR-amplified and cloned into a lentiviral vector LRCherry2.1 (Addgene, 108099). All vector cloning was performed using the In-Fusion Snap Assembly Master Mix (Takara, 638947).

Cas9 sgRNA was expressed in the lentiviral vector LRCherry2.1Tb, retroviral vector pSL21-VEX (Addgene, 158230) or pSL21-mCherry (Addgene, 164410) as previously described[9]. Briefly, sense and antisense DNA oligos were annealed and phosphorylated by T4 Polynucleotide Kinase (NEB, M0201L) and cloned into BsmbI (NEB, R0580) or BbsI (NEB, R0539S) digested LRChe2.1Tb, pSL21-VEX or pSL21 vectors by DNA T4 ligase (NEB, M0202L). To enhance U6 promoter transcription efficiency, an additional G nucleotide was added to the 5′ end of sgRNA oligos if they did not already start with a G. All sgRNA and crRNA sequences used in this study are listed in Supplementary Tables 1 and 2.

Cas protein purification

Cas-CPP proteins, including both Cas9-CPP and opCas12a-CPP variants, were purified, followed by a previously described Cas9 protein purification protocol[47] with minor modifications. Cas-CPP expression vectors were transformed into Rosetta2 (DE3) pLysS competent cells (Millipore, 71403), plated on LB Agar plates containing 100 μg ml^{-1} ampicillin and incubated at 37 °C for 12–16 h. All the transformed bacteria colonies were inoculated into 50 ml of terrific broth (24 g l^{-1} yeast extract, 12 g l^{-1} tryptone, 0.4% glycerol, 2.31 g l^{-1} KH_2PO_4 and 12.54 g l^{-1} K_2HPO_4) with 0.4% glucose, 25 μg ml^{-1} chloramphenicol and 100 μg ml^{-1} ampicillin and continuously cultured at 37 °C shaking at 230 rpm for 4–6 h. The cells were then inoculated into 4 l of terrific broth at 37 °C and shaken at 230 rpm till OD_{600} reached 0.6–0.7. Cells were cooled on ice for 30 min and induced with 0.5 mM IPTG (Millipore, 420322) at 18 °C, shaking at 230 rpm for 14–16 h. Cells were centrifuged at 2,500 *g* for 10 min at 4 °C. Cell pellet was snap frozen on dry ice and stored at −80 °C for further purification.

All the purification steps were carried out either at 4 °C or on ice. Cell pellets were resuspended in B-PER complete bacterial protein extraction reagent (Thermo Fisher Scientific, 89822) containing 500 mM NaCl, 1 mM TCEP (Sigma, C4706), 1 mM PMSF (Sigma, P7626) and complete EDTA-free protease inhibitor cocktail (Sigma, 11873580001) and gently stirred at 4 °C for 30 min. Cell lysates were centrifuged at 16,000 *g* for 30 min at 4 °C. The supernatant containing Cas protein was collected and passed through a 0.22 μM filter before incubating with B-PER washed Strep-Tactin Sepharose resin (IBA Lifesciences, 2-1201-025) for 1 h at 4 °C with gentle rotation according to the manufacturer's instructions. Cas protein-bound beads were washed three times by Cas Wash Buffer (20 mM Tris–HCl, pH 8.0, 500 mM NaCl and 1 mM TCEP), resuspended in SUMO Digestion Buffer (30 mM Tris–HCl, pH 8.0, 500 mM NaCl, 0.15% NP-40 and 1 mM TCEP) with SUMO protease ULP1 (in-house purified) at 80 μg ml^{-1} and rotated overnight at 4 °C for on-bead digestion.

Cas-CPP protein was further purified by ion exchange and size exclusion chromatography. After affinity, ion exchange and size exclusion chromatography purification, the purity of CPP-Cas protein was determined to be >95% by SDS-PAGE gel electrophoresis. It is important to note that lower purity of CPP-Cas protein can be highly toxic to primary cells and may lead to decreased live cell recovery. Briefly, SUMO digestion buffer containing Cas protein was collected and passed through a 0.22-μM filter and loaded onto a HiTrap SP HP (5 ml) cation exchange chromatography column (Cytiva, 17115201) by the AKTA pure protein purification system (Cytiva). The HiTrap SP HP column was washed with 80% of buffer A (20 mM Tris–HCl, pH 8.0, 1 mM TCEP, 5% glycerol and 130 mM NaCl) and 20% of Buffer B (20 mM Tris–HCl, pH 8.0, 1 mM TCEP, 5% glycerol and 2 M NaCl) before eluting Cas protein, with a gradient of Buffer B from 20% to 100%. One milliliter fractions were collected, and Cas-CPP-containing fractions were determined by SDS-PAGE and pooled. Pooled fractions were buffer exchanged with Buffer S200 (10 mM HEPES-Na, pH 7.0, 1 M NaCl, 5 mM $MgCl_2$ and 2 mM TCEP) and concentrated to 0.25–0.5 ml by Amicon Ultra-15 Centrifugal Filter Unit (Millipore, UFC910024) according to the manufacturer's instructions. The concentrated protein was loaded onto a Superdex 200 Increase 10/300 GL (Cytiva, 28990944) size exclusion column and eluted in 0.25 ml fractions by the AKTA pure system. Cas-CPP protein-containing fractions were determined by SDS-PAGE gel electrophoresis, pooled together, buffer exchanged to Cas Storage Buffer (580 mM KCl, 40 mM Tris–HCl, pH 7.5, 20% glycerol, 2 mM TCEP-HCl and 2 mM $MgCl_2$) and concentrated to 50–100 μM.

Purified Cas protein was passed through a 0.22 µM filter, aliquoted and stored at −80 °C.

Assist chemicals and peptides

The chloroquine (Sigma, C6628) and polybrene (Sigma, H9268) were purchased from Sigma. The KALA (AS-65459), Transportan (AS-61256), Penetratin (AS-64885) and Penetrain-Arg (AS-65464) peptides were purchased from AnaSpec, Inc. TAT, HA2 and TAT-HA2 peptides were custom synthesized by Biomatik using the following specifications: HPLC purity of 98%, salt switch to HCl with TFA removal with a guarantee of less than 1% and endotoxin removal with a guarantee of less than 10 EU ml^{-1}. It is important to note that lower purity and quality of peptides can be highly toxic to cells and may result in decreased live cell recovery and inconsistent genome editing efficiency in primary cells. The peptides were reconstituted in PBS at a concentration of 1 mM and passed through a 0.22 µM filter. They were then aliquoted and stored at −80 °C.

Lentiviral production and transduction

Lentivirus was produced as previously described[48]. Briefly, HEK293T cells in 100 mm dishes were transfected with 10 µg of lentiviral plasmid DNA, 5 µg of VSV-G and 7.5 µg of psPAX2 using polyethylenimine (PEI 25 K) at 80 µg ml^{-1} (Polysciences, 23966-100). Lentivirus was collected at 24, 48h and 72 h post-transfection and pooled together. The virus-containing media was centrifuged at 1,800 *g*. The supernatant was passed through a 0.45 µm PVDF filter (Millipore, SLHVR33RS) to remove residual cell debris. To transduce targeted cell lines, 10–50 µl of lentivirus was added to 200,000 cells in 1 ml media with 8 µg ml^{-1} polybrene (Sigma, H9268) in a 12-well plate format. Plates were centrifuged at 600 *g* for 25 min at room temperature. Fresh media was replaced 16 h post-transduction, and transduced cells were enriched via blasticidin selection.

Retrovirus transduction for primary mouse $CD8^+$ T cells

Retrovirus was produced as previously described[9]. Briefly, Plat-E cells in 100 mm dishes were transfected with 10 µg of plasmid DNA, 2 µg of VSV-G and 2 µg of EcoHelper using polyethylenimine at 4 µg ml^{-1}. Retrovirus was collected at 24 hours, 48 hours and 72 hours post-transfection and pooled together. The virus-containing media was centrifuged at 1,800 *g*. The supernatant was passed through a 0.45 µm PVDF filter to remove residual cell debris.

Mouse primary $CD8^+$ T cell retroviral transduction was performed as previously described[9]. $CD8^+$ T cells were isolated from spleens by negative selection using the EasySep Mouse $CD8^+$ T Cell Isolation Kit (STEMCELL, 19853) according to the manufacturer's instructions. Cells were stimulated with 1 µg ml^{-1} anti-mouse CD3ε (Biolegend, 100359), 0.5 µg ml^{-1} anti-mouse CD28 (Biolegend, 102116) and 100 U ml^{-1} recombinant human IL-2 (Peprotech, 200-02) in completed RPMI 1640 media (cRPMI) supplemented with 10% FBS, 20 mM HEPES, 1× NEAA (Thermo Fisher Scientific, 11140050), 1 mM sodium pyruvate (Thermo Fisher Scientific, 11360070), 1× penicillin–streptomycin (Thermo Fisher Scientific, 15140122), 2 mM L-glutamine (Thermo Fisher Scientific, 25030081) and 50 µM β-mercaptoethanol (Thermo Fisher Scientific, 21985023). After 26–28 h of stimulation, 3 million cells in 1 ml cRPMI were transduced with 1 ml of retrovirus in the presence of 4 µg ml^{-1} polybrene and 100 U ml^{-1} IL-2 by spin infection at 2,000 *g* for 75 min at 32 °C. Cells were incubated at 37 °C for 4–6 h and 4 ml of fresh cRPMI with 100 U ml^{-1} IL-2 was added to the culture. Cells were continuously incubated at 37 °C for 20–24 h and then were treated with combinations of Cas9-T6N protein, Cas9-T6N-RNP, opCas12a-RNP and an AP.

CAR T cell transduction and expansion

A lentiviral vector expressing CD19-specific CAR with 4-1BB/CD3ζ domains (GeMCRIS, 0607-793) was derived from CAR19-BB-z, and the lentiviral production was performed similarly as previously described[49]. Briefly, HEK293T cells in 150 mm dishes with 50–60% confluency were transfected with 18 µg pRSV-Rev (Addgene, 12253), 18 µg pMDLg/pRRE (Addgene, 12251), 7 µg VSV-G and 15 µg CAR19-BB-z vector in the presence of 90 µl of Lipofectamine 2000 (Thermo Fisher Scientific, 11668019) in 3 ml of Opti-MEM (Thermo Fisher Scientific, 31985070). Viral supernatant was harvested at 24 and 48 h of post-transduction and centrifuged at 800 *g*. The lentiviral-containing supernatant was filtered through a 0.45 µm PVDF filter and concentrated by ultracentrifugation at 4 °C using Optima XPN-100 ultracentrifuge (Beckman Coulter). Briefly, the supernatant from 24 h post-transduction was centrifuged at 9,000 g for 15 h. The supernatant was then carefully removed, and the lentiviral-containing supernatant from 48 h post-transduction was added and centrifuged at 77,000 g for 2.5 h using a SW 32 Ti rotor. Lentivirus pellet was collected and stored at −80 °C. Lentiviral titer was determined by the percentage of CAR19-positive cells via flow cytometry after SupT1 cells were transduced with a serial dilution of CAR19-BB-z virus.

To generate CAR19 T cells, total human T cells were isolated from normal donor PBMCs (Human Immunology Core at the University of Pennsylvania. Samples are de-identified for compliance with HIPAA rules) by the EasySep Human T Cell Isolation Kit (STEMCELL, 17951) according to the manufacturer's instructions on day 0. Cells were stimulated with Dynabeads Human T-Activator CD3/CD28 for T Cell Expansion and Activation (Thermo Fisher Scientific, 11131D) at beads to cells number ratio of 3:1 and 40 U ml^{-1} recombinant human IL-2 in CTS OpTmizer T Cell Expansion SFM (Thermo Fisher Scientific, A1048501) supplemented with 5% GemCell Human Serum AB (GeminiBio, 100-512) and 4 mM GlutaMax Supplement (Thermo Fisher Scientific, 35050061) at 37 °C. After 24 h (day 1), the CAR19 virus was added to cells at Multiplicity of Infection (MOI) = 2. Cells were continuously cultured for 3 d and then diluted to $0.5-1\times10^6$ ml^{-1} on day 4 postinfection followed by the removal of CD3/CD28 beads. Cells were split every 2–3 d and subcultured at $0.5-1\times10^6$ ml^{-1}.

Cas9-CPP direct delivery

For Cas9-CPP delivery to the mChe reporter cell line experiments, 10 µl of Cas9-CPP protein in storage buffer was first mixed with ~250,000 cells in 100 µl of the completed cell culture media to achieve the indicated concentration, followed by mixing with the indicated APs. Cells were incubated at 37 °C for 30 min, followed by extensive washing with completed media. An additional PBS wash and trypsinization step were performed to remove any cell surface-bound Cas9-CPP protein before FACS sorting or further downstream analyses.

For Cas9-T6N protein delivery to mouse primary $CD8^+$ T cell experiments, sgRNA-transduced $CD8^+$ T cells were FACS sorted, followed by incubation with the indicated concentrations of Cas9-T6N protein and AP at 37 °C for 30 min. Briefly, 350,000–600,000 cells were washed and then resuspended in 50 µl of RPMI supplemented with 1% FBS, 1x penicillin–streptomycin and 50 µM β-mercaptoethanol. Then, cells were mixed with Cas9-T6N protein, followed by mixing with assisting peptide TAT-HA2. Cells were incubated at 37 °C for 30 min, followed by extensive washing using complete cRPMI media and trypsinization to remove cell surface-bound Cas9-T6N protein. Cas9-T6N edited $CD8^+$ T cells were resuspended in 200 µl of complete RPMI supplemented with 100 U ml^{-1} rhIL2.

Cas-CPP-RNP direct delivery

CRISPR guide RNAs were synthesized by IDT and reconstituted to 100 µM using nuclease-free water, and were then diluted to 20 µM as a working solution. The Cas-CPP protein was diluted to 20 µM or 25 µM using RPMI 1640 for mouse primary $CD8^+$ T cells or CTS OpTmizer T Cell Expansion SFM without any serum or supplement for human CAR19 cells, respectively. Before mixing with Cas-RNP, the T cells were washed once with media without any serum or supplement.

To form the RNP, the Cas9-T6N or opCas12a-T8N protein and CRISPR guide RNA (sgRNA for Cas9 and crRNA for opCas12a) were mixed and incubated at room temperature for 15–20 min in vitro. The mixing ratios for the Cas9-RNP complex were 1.25:1 for mouse primary T cells and 1:1 for human CAR19 cells, respectively. The mixing ratio for the opCas12a-RNP was 1.25:1. After formation, the RNP complex was mixed with various concentrations of TAT-HA2 at a 1:1 volume ratio and added to ~240,000 mouse primary $CD8^+$ T cells or 400,000–1,000,000 human CAR19 cells. To prevent precipitation, the RNP complex could also be premixed with the cells before incubation with TAT-HA2 at a 1:1 volume ratio. The cells were then incubated with the Cas-RNP-PAGE at 37 °C for 30 min, followed by extensive washing with complete media. An additional PBS wash and trypsinization step were performed to remove any cell surface-bound Cas-CPP protein before FACS sorting or further downstream analyses.

For $CD34^+$ HSPCs experiments, the opCas12a-RNP was assembled by mixing 25 pmol opCas12a-T8N and 20 pmol chemically modified crRNA (IDT) for 15 min at room temperature in 10 µl of 1x Opti-MEM Reduced Serum Medium. The opCas12-RNP complex was then mixed with 10 µl of 100-µM AP peptide and incubated for 5 min at room temperature. Approximately 100,000 human primary $CD34^+$ HSPC-derived progenitors were washed twice with 1x Opti-MEM Reduced Serum Medium and incubated with the opCas12a-RNP-PAGE for 30 min at 37 °C, followed by thorough washing with culture media.

Multiplex genome editing

For the sequential multiplex genome editing experiment, the opCas12a-RNP was formed as described previously. Notably, 1 million CAR19 cells were incubated with opCas12a-RNP-PAGE loaded with the first crRNA for 30 min at 37 °C, and thoroughly washed with complete media. After 2 d, 1 million PAGE-edited CAR19 cells from the first crRNA were incubated with opCas12a-RNP-PAGE loaded with the second crRNA for 30 min at 37 °C, and thoroughly washed with complete media. For the simultaneous multiplex genome editing, opCas12a-T8N-RNP was created by mixing opCas12a-T8N protein with individual crRNA at a ratio of 1.25:1 and then incubated for 15–20 min at room temperature. TAT-H2A was then added to the RNP complex at a 1:1 volume ratio, resulting in a final concentration of 5 µM opCas12a-T8N-RNP and 25 µM TAT-HA2. The opCas12a-RNP-PAGE containing different crRNAs were combined at a 1:1 volume ratio and then mixed with either 1 million CAR19 cells or $CD34^+$ HSPCs. The cells were incubated with the mixture of opCas12a-RNP-PAGE for 30 min at 37 °C, and thoroughly washed with complete media.

Flow cytometry and sorting

To evaluate the gene editing efficiency of Cas9-CPP and Cas9-PAGE in the mChe reporter cells, the mChe-positive cell population was monitored over a time course using either a Guava easyCyte HT (Millipore) or a BD Accuri C6 Plus Flow Cytometer (BD Biosciences). To evaluate gene editing efficiency of Cas9-CPP and Cas9/opCas12a-PAGE in mouse primary T cells, cells were stained with an antibody against the targeted protein and the Live/Dead Fixable Aqua Dead Cell Stain Kit (Thermo Fisher Scientific, L34966) at 4 °C for 30 min, followed by fixation at 4 °C for 10 min with Stabilizing Fixative (BD Biosciences, 338036). To evaluate the efficiency of gene editing with either Cas9-RNP-PAGE or opCas12a-RNP-PAGE in human CAR19 cells, the cells were first treated with Biotin-Goat anti-mouse IgG F(ab)2 (1:50, Jackson ImmunoResearch, 115-065-072) for 20 min at room temperature, followed by a single wash with FACS buffer (3% FBS and 2 mM EDTA in PBS). The cells were then stained with APC streptavidin (1:100; Biolegend, 405207) together with the indicated target protein antibodies for 20 min at room temperature, and finally fixed at 4 °C for 10 min with Stabilizing Fixative (BD Biosciences, 338036). Target protein expression was analyzed on a BD LSRFortessa and FlowJo (10.8.1).

To sort human CAR19-positive cells, cells were first stained with Biotin-Goat anti-mouse IgG $F(ab)_2$ (1:50; Jackson ImmunorResearch, 115-065-072) for 20 min at room temperature and were then washed once with FACS buffer (3% FBS and 2 mM EDTA in PBS). Cells were then stained with APC streptavidin (1:100; Biolegend, 405207) for 20 min at room temperature. Cells were washed twice with FACS buffer and resuspended in cold FACS buffer at 10–15 million cells per ml and sorted on a MoFlo Astrios EQ (Beckman Coulter) at 4 °C using a 100-micron nozzle. Sorted cells were collected in cold completed CTS OpTmizer T Cell Expansion SFM during sorting and washed once with the completed media before ex vivo culture. Cells were rested at 37 °C for 4–24 h before Cas-RNP-PAGE incubation.

$sgRNA^+$ mouse primary $CD8^+$ T cell sorting was performed as previously described with minor modifications[9]. Briefly, cells were resuspended in prewarmed FACS buffer at 37 °C at a concentration of 10–15 million cells per ml and sorted on a BD FACS Jazz at room temperature using a 100-micron nozzle. Sorted cells were collected in 37 °C prewarmed cRPMI media supplemented with 100 U ml^{-1} rhIL2 during sorting and washed once with 37 °C prewarm complete RPMI before ex vivo culture. Cells were rested at 37 °C for 4–6 h before Cas9-PAGE incubation.

To sort $Cas9^+$ cells after incubation with Cas-PAGE, cells were washed extensively with media, followed by trypsinization to remove all remaining cell surface-bound Cas9-CPP protein. Briefly, 1.2 million cells were washed once with RPMI media and resuspended in 0.25% trypsin at 37 °C for 5 min. Trypsin was neutralized by adding warm cRPMI, followed by 400 U ml^{-1} DNase I treatment at 37 °C for 3 min to reduce cell clumping. Cells were then washed twice with cRPMI. Cells were resuspended in either FACS buffer or cRPMI with 100 U ml^{-1} rhIL2 and rested at 37 °C for 20–60 min before sorting.

LIVE/DEA Fixable Aqua Dead Cell Stain Kit (L34966, 1:600), APC anti-mouse CD90.2 antibody (17-0902-81, 1:600) and PE mouse anti-human CD45 (12-0459-41, 1:100) were purchased from Thermo Fisher Scientific. APC anti-mouse CD45.2 antibody (109814, 1:100), Brilliant Violet 421 anti-human TCR α/β (306721, 1:100) and APC/cyanine7 anti-human CD45 (304014, 1:100) were purchased from BioLegend. PE mouse anti-human β2-microglobulin (551337, 1:200) was purchased from BD.

Live cell counting

Live cells were counted by a Countess Automated Cell Counter (Invitrogen) or determined using flow cytometry analysis based on FSC and SSC gating. For mouse and human primary T cells, cells were mixed with trypan blue and counted via a hemocytometer before activation or immediately after Cas-PAGE incubation. Live cells were counted 6 h after electroporation or Cas-RNP-PAGE via hemocytometer to compare the cellular toxicity.

Cas9-PAGE in mouse primary $CD8^+$ T cells for in vivo study

P14 $CD8^+$ T cells from two congenically distinct donor mice were isolated and activated in vitro for 24–28 h as previously described[9]. Following activation, $CD8^+$ P14 cells of one congenic mouse were transduced with retrovirus expressing either sgPdcd1_IG44 or sgThy1_IG1, while $CD8^+$ P14 cells of a second congenic mouse were transduced with negative control sg*Ano9*. After 20 h sgRNA retroviral transduction, cells were incubated with Cas9-PAGE (5 µM Cas9-T6N and 25 µM of TAT-HA2) at 37 °C for 30 min. Cells were washed with cRPMI media and treated with trypsin to remove cell surface-bound Cas9-T6N protein. P14 $CD8^+$ T cells expressing the sgRNA RV reporter (mCherry or Vex) and Cas9 (GFP) were sorted on a BD FACS Aria (100 µM nozzle, 37 °C). Sorted cells were washed twice in RPMI and resuspended in RPMI supplemented with 1% FBS at 2.5×10^5 cells per ml. Experimental sgRNA-transduced and sg*Ano9*-transduced P14 cells were mixed at a 1:1 ratio, and the ratio was confirmed by flow cytometry. Before 2 d, 50,000 P14 $CD8^+$ T cells were adoptively transferred to recipient mice of a third congenic mouse

infected with LCMV clone 13. On days 8, 15, 22 and 30 after adoptive transfer, blood or spleen were collected and stained for flow cytometry. Samples were analyzed in FlowJo (10.8.1).

Flow cytometry for in vivo study

Mouse PBMC were isolated from whole blood by histopaque gradient (650 g, 20 min, room temperature; Histopaque-1083, Sigma). Spleens were mechanically disrupted over a 70 µm filter, followed by ACK lysis and counted. All samples were resuspended in FACS buffer (FACS buffer; DPBS + 3% FCS + 2 mM EDTA) before staining. Samples were washed in PBS, incubated with LIVE/DEAD Fixable NIR Dead cell stain kit (15 min, room temperature; Thermo Fisher Scientific, L34975) and then washed in FACS buffer. Samples were stained with antibody cocktail in Brilliant Stain buffer (BD Biosciences, 566349) for 30 min at 4 °C, and washed twice in FACS buffer. Samples were fixed (3X Stabilizing Fixative; BD Biosciences, 338036) for 15 min at room temperature and run immediately on a BD LSRII. Samples were analyzed in FlowJo (10.8.1). Statistical significance for flow cytometry data was calculated using statistical tests indicated in legends using GraphPad Prism (9.4.1).

Pacific Blue anti-mouse LY108 antibody (134608, 1:100), BV605 anti-mouse CD45.2 antibody (109841, 1:100), BV785 anti-mouse CD45.1 antibody (110743, 1:200), BV650 anti-mouse CX3CR1 antibody (149033, 1:100), BV711 anti-mouse CD44 antibody (103057, 1:1,000), BV785 anti-mouse CD44 antibody (103059, 1:2,000), PE-Cy7 anti-mouse PD-1 antibody (109110; 1:100) and AF700 anti-mouse CD90.2 antibody (105320, 1:100) were purchased from BioLegend. Gp33 tetramer (PE, 1:400) was generated in-house. BB700 anti-mouse KLRG1 (742199, 1:100) and PE-CF594 anti-mouse CD127 antibody (562418, 1:100) were purchased from BD Biosciences. PE-Cy5 anti-mouse CD45.1 antibody (15-0453-82, 1:600), APC anti-mouse CD8 antibody (17-0081-81, 1:600), APC-eF780 anti-mouse CD4 antibody (47-0042-82, 1:100) and B220 anti-mouse APC-eF780 antibody (47-0452-82, 1:100) were purchased from Invitrogen.

Cell fractionation and western blot

To evaluate the Cas9-T6N uptake and cellular localization, approximately 3.5 million EL4 cells were incubated with either 5 µM Cas9-T6N only or 5 µM Cas9-T6N and 75 µM TAT-HA2 in DMEM media supplemented with 10% FBS at 37 °C for 30 min. Cells were washed once with PBS, trypsinized for 10 min at 37 °C, washed and resuspended in DMEM supplemented with 10% FBS. Cells were then rested at 37 °C for 4 h. Nuclear and cytosolic fractions were separated using a Nuclear Extraction Kit (Abcam, ab113474) according to the manufacturer's instructions. The whole-cell lysates were prepared from direct lysing of the cells using a 25-mm syringe in Laemmli sample buffer (Bio-Rad) containing 5% b-mercaptoethanol. Protein extracts were boiled at 95 °C for 7 min and were separated by electrophoresis before being transferred to a nitrocellulose membrane as previously described[48]. Membranes were first blocked in 5% milk and TBST at room temperature for 30 min. Then, membranes were incubated with primary antibodies at a 1:1,000 dilution in 5% milk and TBST at 4 °C overnight with shaking. The following morning, membranes were incubated with secondary antibodies at a 1:10,000 dilution in Odyssey Blocking Buffer (LI-COR Biosciences, 927-40000). Blots were imaged on an LI-COR Odyssey, and the band intensities were quantified using Image Studio (5.2.5).

The primary and secondary antibodies used for the western blotting were anti-Cas9 antibody (7A9-3A3; Abcam, ab191468), anti-Lamin B1 (Abcam, ab16048), anti-α-Tubulin (Cell Signaling, 2148), anti-Rabbit (LI-COR Biosciences, 925-32211) and anti-Mouse (Invitrogen, A-21058).

Electroporation of Cas-RNP

For CAR19 cell experiments, Cas-RNP was electroporated into the cells using the Amaxa 4D Nucleofector System (Lonza) and the P3 Primary Cell 4D Nucleofector X Kit S (Lonza, V4XP-3032) following the manufacturer's instructions. The RNP was assembled by mixing opCas12a-T8N and crRNA at a 1.25:1 molar ratio for 15–20 min at room temperature. The P3 Primary Cell Solution and Supplement 1 were mixed at a 4.5:1 volume ratio, then added to the RNP, resulting in a total volume of 20 µl and a final RNP concentration of 5 µM. One million CAR19 cells were washed with PBS and then resuspended in 20 µl of P3 Primary Cell Solution that contained the RNP. The cells were transferred to 16-well Nucleocuvette Strips and electroporated with the program EO-115 designed for stimulated human T cells. Notably, 80 µl of prewarmed cell culture media was added to the cuvette immediately after electroporation. The cells were gently resuspended and transferred to a 24-well plate containing 900 µl of prewarmed media for continuous culture.

For $CD34^+$ HSPCs experiments, the Cas12a-RNP was assembled by mixing 63-pmol Alt-R A.s.Cas12a Ultra (from IDT) and 80 pmol chemically modified crRNA (from IDT) for 15 min at room temperature. Approximately 100,000 human primary $CD34^+$ HSPC-derived progenitors from phase 1 differentiation were washed with PBS and then resuspended in P3 Primary Cell Solution that contained the Cas12a-RNP. The cells were electroporated with Cas12a-RNP using the 4D Nucleofector from Lozano (program DZ-100) following the manufacturer's instructions.

RNA-seq and data analysis

To profile transcriptional changes using RNA-seq, 0.5 to 2 million CAR19 cells were collected 6 h and 3 d post-treatment with either opCas12a-RNP-PAGE or electroporation. The cells were washed once with PBS and then suspended in 0.5 ml of TRIzol (Thermo Fisher Scientific, 15596018). RNA was extracted using the RNA Clean and Concentrator-5 kit (ZYMO, R1013) following the manufacturer's instructions. mRNA was isolated from 500 ng of RNA using the NEBNext Poly(A) mRNA Magnetic Isolation Module (NEB, E7490L). The next-generation sequencing libraries were constructed using the NEBNext Ultra II Directional RNA Library Prep Kit (NEB, E7760L) following the manufacturer's instructions. The RNA libraries were pooled and sequenced using the NextSeq 500/550 High Output Kit (75 cycles) v2.5 kit (Illumina, 20024906) on the NextSeq 550 platform (Illumina) using paired-end sequencing.

To analyze the RNA-seq data, the FASTQ files were processed using STAR v2.7.1a and aligned to the hg38 Gencode reference genome[50]. The read counts of each gene were quantified by STAR using the '–quantMode GeneCounts' parameter. To adjust for donor-to-donor variations, we modeled the donor batch effects in the DESeq2 model design by setting the design equal to '~donor + condition' in the DESeqDataSetFromMatrix() function. Normalized read counts were generated using DESeq2, and batch-corrected read counts were then generated using the limma::removeBatchEffect() function with the batch modeled as the donor[51]. Principal component analysis plots were generated using the R function prcomp, and differentially expressed genes were identified using DESeq2 with filters of absolute $\log_2$ fold change greater than 0.5 and an adjusted $P < 0.01$. MA plots of differential gene expression were generated using the plotMA function.

CAR19 and NALM6 coculture experiment

To evaluate the cytotoxic capacity of PAGE-edited CAR19 cells, coculture killing experiments with CAR19 and NALM6 were performed. Briefly, CAR19 cells were subjected to a 30-min incubation with opCas12-RNP-PAGE loaded with crNeg or mock treatment (without opCas12-RNP-PAGE). PAGE-treated CAR19 cells, either 6 h or 10 d post-treatment, were cocultured with NALM6 tumor cells for 17 h, using various effector (CAR19)-to-target (NALM6) cell ratios in 200 µl of completed OpTmizer T Cell Expansion SFM without rhIL2. To determine the live cell population of NALM6 after 17 h of coculture with PAGE-edited CAR19 cells, 10 µl of CountBright Absolute Counting Beads (Thermo Fisher Scientific, C36950) was added to the cell culture, followed by flow cytometry analysis using a BD LSRFortessa. At least 2,500 bead events were recorded.

On-target and off-target of Cas9-RNP-PAGE

To evaluate the on-target and off-target gene editing efficiency of Cas9-RNP-PAGE, CAR19 cells were incubated for 30 min with a 1:1 molar ratio of Cas9-T6N and either sgEMX1 or sgFANCF in the presence of 75 μM TAT-HA2. The cells were then washed thoroughly with complete media. After 10 d treatment, 2 million PAGE-edited CAR19 cells were subjected to genomic DNA extraction using the Quick-DNA Miniprep Plus Kit (ZYMO, D4068). DNA was amplified from 100 ng of the extracted genomic DNA at the on-target site and two well-established off-target sites for each sgRNA. The purified PCR products were used to prepare next-generation sequencing libraries with the NEBNext Ultra II DNA Library Prep Kit (NEB, E7760L) and were sequenced on the MiSeq system (Illumina) using the MiSeq Reagent Nano Kit v2 (300 cycles; Illumina, MS-103-1001) in paired-end sequencing.

To analyze the data, the raw reads were processed as follows: first, they were demultiplexed using the MiSeq Reporter software. Then, FastQC v0.11.9 was used to evaluate the quality of the demultiplexed reads. Low-quality reads (with a Phred quality score of less than 28) were removed, and adapters were trimmed using Trim Galore v0.6.6. The processed reads were analyzed using CRISPResso2 with default settings, allowing for the classification of unmodified reads within the sgRNA recognition site versus aggregate modified, edited reads[52]. The percentage of indels was calculated by dividing the number of modified reads by the total number of reads at the target site (which includes both unmodified and modified reads).

$CD34^+$ culture

Frozen G-CSF-mobilized $CD34^+$ HSPCs isolated from the peripheral blood of healthy human donors were obtained from the Co-Operative Center for Excellence in Hematology at the Fred Hutchinson Cancer Research Center and were cultured as described previously[35]. Briefly, the cells were thawed in PBS with 1% FBS at room temperature according to the manufacturer's instructions. The $CD34^+$ HSPCs were then differentiated into erythroid cells using a three-phase erythroid differentiation protocol[35]. The growth medium was prepared using 1× IMDM according to the following instructions: Phase I, 100 ng ml^{-1} human SCF, 5 ng ml^{-1} IL-3, 3 IU ml^{-1} Epoetin alfa, 2.5% human serum (Sigma, I9278), 10 ng ml^{-1} heparin, 10 mg ml^{-1} insulin and 250 mg ml^{-1} holo-transferrin; Phase II, 100 ng ml^{-1} human SCF, 3 IU ml^{-1} Epoetin alfa, 2.5% human serum, 10 ng ml^{-1} heparin, 10 mg ml^{-1} insulin and 250 mg ml^{-1} holo-transferrin; Phase III, 3 IU ml^{-1} Epoetin alfa, 2.5% human serum, 10 ng ml^{-1} heparin, 10 mg ml^{-1} insulin and 1.25 mg ml^{-1} holo-transferrin.

qRT-PCR for gene expression analysis

Total RNA from primary erythroid cells at day 13 of differentiation was extracted with RNeasy Plus Mini Kit (Qiagen, 74136). To remove genomic DNA, the extracted RNA was subjected to in-column DNase I digestion. 500 ng of total RNA was converted into cDNA using the iScript Master Mix (Bio-Rad, 1708841). Quantitative PCR was performed using SYBR Green (Invitrogen, 4367660), and the data were normalized to AHSP. A list of primers used for qRT-PCR can be found in Supplementary Tables 1 and 2.

HbF flow cytometry and analysis

At day 13 of the differentiation of $CD34^+$ HSPCs into erythroid cells, 1 million primary erythroid cells were washed with PBS and then fixed with 0.05% glutaraldehyde (Sigma Aldrich, G6257) for 10 min. The cells were permeabilized with 0.1% Triton for 3 min at room temperature, and then stained with an APC-conjugated HbF polyclonal antibody (Novus Biological, NB110-41084; 1:2,000) for 15 min on ice. Flow cytometry analysis was performed using a BD FACSCanto instrument and analyzed using BD FACSDiva (8.0.2).

TIDE assay and indel analysis

To evaluate on-target mutagenesis, the Tracking of Indels by Decomposition (TIDE) assay was performed on at least 4×10^5 cells after incubation with Cas9-PAGE or opCas12a-RNP-PAGE. TIDE PCR primers were designed as previously described[53]. The *BCL11A* +58 kb enhancer region was amplified through a two-step PCR reaction to obtain a selective on-target amplicon[54]. Genomic DNA was isolated using Quick-DNA Miniprep Plus Kit (ZYMO, D4068), and 150 ng of genomic DNA was used to amplify approximately 300–400 bp upstream and downstream of the sgRNA or crRNA targeting sites. The PCR product was purified using a DNA Clean & Concentrator-5 kit (ZYMO, D4014) or a Zymoclean Gel DNA Recovery Kit (ZYMO, D4008) after agarose gel extraction. Notably, 50 ng PCR production was sent for Sanger sequencing (Genewiz). For mouse and human primary T cell experiments, the percentage of guide RNA-induced indel was evaluated by TIDE version 3.3.0 with the following parameters: decomposition window −200 and +200 bp of the expected cut site; indel size range 1–50 bp; *P* value threshold 0.05. For primary human $CD34^+$ HSPCs, gene editing efficiency was determined by DECODR v3.0 (https://decodr.org/). A list of primers used for TIDE assay can be found in Supplementary Tables 1 and 2.

Reporting summary

Further information on research design is available in the Nature Portfolio Reporting Summary linked to this article.

Data availability

The accession numbers for the RNA-seq dataset in this study is GSE223805(ref. 55). The GRCh38/hg38 human reference genome is publicly available. Key plasmids, Cas9-T6N and Cas12a-T8N have been deposited at Addgene (plasmid ID, 199604–199605). Source data are provided with this paper, including unprocessed Western blots.

References

46. Pauken, K. E. et al. Epigenetic stability of exhausted T cells limits durability of reinvigoration by PD-1 blockade. *Science* **354**, 1160–1165 (2016).
47. Gootenberg, J. S. et al. Nucleic acid detection with CRISPR-Cas13a/C2c2. *Science* **356**, 438–442 (2017).
48. Cao, Z. et al. ZMYND8-regulated IRF8 transcription axis is an acute myeloid leukemia dependency. *Mol Cell* **81**, 3604–3622 (2021).
49. Milone, M. C. et al. Chimeric receptors containing CD137 signal transduction domains mediate enhanced survival of T cells and increased antileukemic efficacy in vivo. *Mol. Ther.* **17**, 1453–1464 (2009).
50. Dobin, A. et al. STAR: ultrafast universal RNA-seq aligner. *Bioinformatics* **29**, 15–21 (2013).
51. Ritchie, M. E. et al. Limma powers differential expression analyses for RNA-sequencing and microarray studies. *Nucleic Acids Res.* **43**, e47 (2015).
52. Clement, K. et al. CRISPResso2 provides accurate and rapid genome editing sequence analysis. *Nat. Biotechnol.* **37**, 224–226 (2019).
53. Brinkman, E. K., Chen, T., Amendola, M. & van Steensel, B. Easy quantitative assessment of genome editing by sequence trace decomposition. *Nucleic Acids Res.* **42**, e168 (2014).
54. Wu, Y. et al. Highly efficient therapeutic gene editing of human hematopoietic stem cells. *Nat. Med.* **25**, 776–783 (2019).
55. Zhang, Z. et al. Efficient engineering of human and mouse primary cells using peptide-assisted genome editing. NCBI. https://www.ncbi.nlm.nih.gov/geo/query/acc.cgi?acc=GSE223805 (2023).

Acknowledgements

We thank M. Szurgot and R. Marmorstein (Department of Biochemistry and Biophysics, University of Pennsylvania) for sharing the protease ULP1 expression vector and purification protocol. We also thank the staff at the Flow Cytometry Core Laboratory of Children's Hospital of Philadelphia. G.A.B. acknowledges NIH/NHLBI (R01-HL119479). R.M.K. acknowledges NIH (R01-GM138908). E.J.W. acknowledges support

from the NIH (AI105343, AI082630, AI108545, AI155577, AI149680 and U19AI082630), funding from the Allen Institute for Immunology and the Parker Institute for Cancer Immunotherapy. Work in the Wherry lab is supported by the Parker Institute for Cancer Immunotherapy. S.L.B. acknowledges NIH/NCI (R35-CA263922). J.S. acknowledges NIH/NCI (R01-CA258904).

Author contributions

Z.Z., E.J.W., S.L.B. and J.S. conceived and developed the Peptide-Assisted Genome Editing (PAGE) approach and designed the research. Z.Z., A.E.B., D.R., K.Q., Z.C., S.M., H.H., C.A.K., P.F.B. and J.B.P. performed experiments and analyzed the data. G.A.B., R.M.K., E.J.W., S.L.B. and J.S. supervised the research. Z.Z. and J.S. drafted the manuscript. Z.Z., A.E.B., G.A.B., R.M.K., E.J.W., S.L.B. and J.S. reviewed and edited the manuscript with input from all authors. All authors read and approved the final manuscript.

Competing interests

Z.Z., A.E.B., Z.C., J.B.P., R.M.K., E.J.W., S.L.B. and J.S. through the University of Pennsylvania have filed a patent application on aspects of this work. E.J.W. is a member of the Parker Institute for Cancer Immunotherapy which supported this study. E.J.W. is an advisor for Danger Bio, Janssen, New Limit, Marengo, Pluto Immunotherapeutics Related Sciences, Santa Ana Bio, Synthekine and Surface Oncology. E.J.W. is a founder of and holds stock in Surface Oncology, Danger Bio and Arsenal Biosciences. R.M.K. is on the Scientific Advisory Board for Life Edit, Inc.

Additional information

Supplementary information The online version contains supplementary material available at https://doi.org/10.1038/s41587-023-01756-1.

Correspondence and requests for materials should be addressed to E. John Wherry, Shelley L. Berger or Junwei Shi.

Peer review information *Nature Biotechnology* thanks Meisam Kararoudi and the other, anonymous, reviewer(s) for their contribution to the peer review of this work.

Reprints and permissions information is available at www.nature.com/reprints.

nature portfolio

Corresponding author(s): Junwei Shi

Last updated by author(s): Mar 20, 2023

Reporting Summary

Nature Portfolio wishes to improve the reproducibility of the work that we publish. This form provides structure for consistency and transparency in reporting. For further information on Nature Portfolio policies, see our Editorial Policies and the Editorial Policy Checklist.

Statistics

For all statistical analyses, confirm that the following items are present in the figure legend, table legend, main text, or Methods section.

n/a	Confirmed
☐	☒ The exact sample size (*n*) for each experimental group/condition, given as a discrete number and unit of measurement
☐	☒ A statement on whether measurements were taken from distinct samples or whether the same sample was measured repeatedly
☐	☒ The statistical test(s) used AND whether they are one- or two-sided *Only common tests should be described solely by name; describe more complex techniques in the Methods section.*
☒	☐ A description of all covariates tested
☒	☐ A description of any assumptions or corrections, such as tests of normality and adjustment for multiple comparisons
☐	☒ A full description of the statistical parameters including central tendency (e.g. means) or other basic estimates (e.g. regression coefficient) AND variation (e.g. standard deviation) or associated estimates of uncertainty (e.g. confidence intervals)
☐	☒ For null hypothesis testing, the test statistic (e.g. *F*, *t*, *r*) with confidence intervals, effect sizes, degrees of freedom and *P* value noted *Give P values as exact values whenever suitable.*
☒	☐ For Bayesian analysis, information on the choice of priors and Markov chain Monte Carlo settings
☒	☐ For hierarchical and complex designs, identification of the appropriate level for tests and full reporting of outcomes
☒	☐ Estimates of effect sizes (e.g. Cohen's *d*, Pearson's *r*), indicating how they were calculated

Our web collection on statistics for biologists contains articles on many of the points above.

Software and code

Policy information about availability of computer code

Data collection	Millipore Guava easyCyte HT, BD Accuri C6 Plus Flow Cytometer, BD LSRFortessa, BD LSR II, BD FACSCanto, Illumina MiSeq, Illumina NextSeq 550, Invitrogen Countess II Automated Cell Counters, Applied Biosystems ViiA 7, and LI-COR Odyssey Imagers
Data analysis	FlowJo 10.8.1, BD FACSDiva 8.0.2, GraphPad Prism 9.4.1, DECODR v3.0, STAR v2.7.1a, DESeq2, FastQC v0.11.9, Trim Galore v0.6.6, Image Studio 5.2.5, and CRISPResso2

For manuscripts utilizing custom algorithms or software that are central to the research but not yet described in published literature, software must be made available to editors and reviewers. We strongly encourage code deposition in a community repository (e.g. GitHub). See the Nature Portfolio guidelines for submitting code & software for further information.

Data

Policy information about availability of data

All manuscripts must include a data availability statement. This statement should provide the following information, where applicable:

- Accession codes, unique identifiers, or web links for publicly available datasets
- A description of any restrictions on data availability
- For clinical datasets or third party data, please ensure that the statement adheres to our policy

The RNA-seq data in this study will be available from NCBI Gene Expression Omnibus under accession GSE223805.
The GRCh38/hg38 human reference genome is publicly available

Human research participants

Policy information about studies involving human research participants and Sex and Gender in Research.

Reporting on sex and gender	n/a
Population characteristics	n/a
Recruitment	n/a
Ethics oversight	n/a

Note that full information on the approval of the study protocol must also be provided in the manuscript.

Field-specific reporting

Please select the one below that is the best fit for your research. If you are not sure, read the appropriate sections before making your selection.

☒ Life sciences ☐ Behavioural & social sciences ☐ Ecological, evolutionary & environmental sciences

For a reference copy of the document with all sections, see nature.com/documents/nr-reporting-summary-flat.pdf

Life sciences study design

All studies must disclose on these points even when the disclosure is negative.

Sample size	Samples from cell lines were evaluated in triplicate or quadruplicate. For experiments with primary human cells, individual donors were treated as individual replicates with 2-3 donors per experiment. 5-10 individual mice were used per condition and time point for in vivo studies based on our previous experience on similar work (Chen et al.,Cell 2021). No sample-size calculations were performed. Sample sizes in all experiments were determined to be sufficient due to effect size, level of variation within groups, consistency of measurable differences among groups, and statistical indicators of reproducibility.
Data exclusions	No data was excluded.
Replication	Biological replicate experiments from cell lines were performed using cells with different passage number spanning days to weeks; Biological replicate experiments from primary cells were performed using at least 2 different donors; data from in vivo mouse experiments represent two independent biological replicate experiments with 5-10 individual mice each replicate.
Randomization	For the in vivo mouse experiments, mice were randomized by sex, cage and littermates. For ex vivo and in vitro studies, random allocation is not relevant.
Blinding	Investigators were not blinded to group allocation during data collection or analysis. Blinding was not relevant to this study because assignment of data values to samples was automated (e.g. flow cytometry method programs) and not based on subjective investigator assessments or assigning values from an analog measurement device.

Reporting for specific materials, systems and methods

We require information from authors about some types of materials, experimental systems and methods used in many studies. Here, indicate whether each material, system or method listed is relevant to your study. If you are not sure if a list item applies to your research, read the appropriate section before selecting a response.

Materials & experimental systems

n/a	Involved in the study
☐	☒ Antibodies
☐	☒ Eukaryotic cell lines
☒	☐ Palaeontology and archaeology
☐	☒ Animals and other organisms
☒	☐ Clinical data
☒	☐ Dual use research of concern

Methods

n/a	Involved in the study
☒	☐ ChIP-seq
☐	☒ Flow cytometry
☒	☐ MRI-based neuroimaging

Antibodies

Antibodies used

APC anti-mouse CD90.2 clone 53-2.1 (cat# 17-0902-81, 1:600), PE Mouse Anti-Human CD45 clone HI30 (cat# 12-0459-41, 1:100), CD45.1 Monoclonal Antibody PE-Cy5 clone A20 (cat# 15-0453-82, 1:600), CD8a Monoclonal Antibody APC clone 53-6.7 (cat# 17-0081-81, 1:600), CD4 Monoclonal Antibody APC-eFluor™ 780 clone RM4-5 (cat# 47-0042-82, 1:100), CD45R (B220) Monoclonal Antibody APC-eFluor™ 780 clone RA3-6B2 (cat# 47-0452-82, 1:100), and Goat anti-Mouse IgG (H+L) Highly Cross-Adsorbed Secondary Antibody (cat# A-21058, 1:10,000) were purchased from Thermo. PE Mouse Anti-Human β2-Microglobulin clone TÜ99 (cat# 551337, 1:200), BB700 Hamster Anti-Mouse KLRG1 clone 2F1 (cat# 742199, 1:100), and PE-CF594 Mouse Anti-Mouse IL-17F/CD127 clone O79-289 (cat# 562418, 1:100) were purchased from BD Biosciences. APC anti-mouse CD45.2 Antibody clone 104 (cat# 109814, 1:100), Brilliant Violet 421 anti-human TCR α/β clone IP26 (cat# 306721, 1:100), APC/Cyanine7 anti-human CD45 clone HI30 (cat# 304014, 1:100), Pacific Blue™ anti-mouse Ly108 Antibody clone 330-AJ (cat# 134608, 1:100), Brilliant Violet 605™ anti-mouse CD45.2 Antibody clone 104 (cat# 109841, 1:100), Brilliant Violet 785™ anti-mouse CD45.1 Antibody clone A20 (cat# 110743, 1:200), Brilliant Violet 650™ anti-mouse CX3CR1 Antibody clone SA011F11 (cat# 149033, 1:100), Brilliant Violet 711™ anti-mouse/human CD44 Antibody clone IM7 (cat# 103057, 1:1,000), Brilliant Violet 785™ anti-mouse/human CD44 Antibody clone IM7 (cat# 103059, 1:2,000), PE/Cyanine7 anti-mouse CD279 (PD-1) Antibody clone RMP1-30 (cat# 109110, 1:100), Alexa Fluor® 700 anti-mouse CD90.2 clone (Thy1.2) Antibody clone 30-H12(cat# 105320, 1:100), and APC streptavidin (cat# 405207, 1:100) were purchased from Biolegend. Biotin-Goat anti-mouse IgG F(ab)2 (cat# 115-065-072, 1:50) was purchased from Jackson-immunoresearch. Anti-CRISPR-Cas9 antibody clone 7A9-3A3(cat# ab191468, 1:1,000) and Anti-Lamin B1 polyclonal antibody (cat# ab16048, 1:1,000) were purchased from Abcam. α/β-Tubulin polyclonal antibody (cat# 2148, 1:1,000) was purchased from Cell Signaling. Anti-IgG Goat Polyclonal Antibody (cat# 925-32211, 1:10,000) was purchased from LI-COR Biosciences. Fetal Hemoglobin Polyclonal Antibody (cat# NB110-41084, 1:2,000) was purchased from Novus Biological and conjugated with APC in house.

Validation

APC anti-mouse CD90.2 clone 53-2.1 (cat# 17-0902-81, 1:600), PE Mouse Anti-Human CD45 clone HI30 (cat# 12-0459-41, 1:100), APC anti-mouse CD45.2 Antibody clone 104 (cat# 109814, 1:100), Brilliant Violet 421 anti-human TCR α/β clone IP26 (cat# 306721, 1:100), APC/Cyanine7 anti-human CD45 clone HI30 (cat# 304014, 1:100), PE Mouse Anti-Human β2-Microglobulin clone TÜ99 (cat# 551337, 1:200), PE/Cyanine7 anti-mouse CD279 (PD-1) Antibody clone RMP1-30 (cat# 109110, 1:100), and Alexa Fluor® 700 anti-mouse CD90.2 clone (Thy1.2) Antibody clone 30-H12(cat# 105320, 1:100) were validated by flow cytometry by staining target gene CRISPR KO cells in this study.

CD45.1 Monoclonal Antibody PE-Cy5 clone A20 (cat# 15-0453-82, 1:600), CD8a Monoclonal Antibody APC clone 53-6.7 (cat# 17-0081-81, 1:600), CD4 Monoclonal Antibody APC-eFluor™ 780 clone RM4-5 (cat# 47-0042-82, 1:100), CD45R (B220) Monoclonal Antibody APC-eFluor™ 780 clone RA3-6B2 (cat# 47-0452-82, 1:100), BB700 Hamster Anti-Mouse KLRG1 clone 2F1 (cat# 742199, 1:100), PE-CF594 Mouse Anti-Mouse IL-17F/CD127 clone O79-289 (cat# 562418, 1:100), Pacific Blue™ anti-mouse Ly108 Antibody clone 330-AJ (cat# 134608, 1:100), Brilliant Violet 605™ anti-mouse CD45.2 Antibody clone 104 (cat# 109841, 1:100), Brilliant Violet 785™ anti-mouse CD45.1 Antibody clone A20 (cat# 110743, 1:200), Brilliant Violet 650™ anti-mouse CX3CR1 Antibody clone SA011F11 (cat# 149033, 1:100), Brilliant Violet 711™ anti-mouse/human CD44 Antibody clone IM7 (cat# 103057, 1:1,000), and Brilliant Violet 785™ anti-mouse/human CD44 Antibody clone IM7 (cat# 103059, 1:2,000) were validated by flow cytometry by staining cells with both positive and negative populations.

Anti-CRISPR-Cas9 antibody clone 7A9-3A3(cat# ab191468, 1:1,000) was validated by Western Blot by probing cells with or without TAT-HA2 treatment in this study and in NOMO1 cells with Cas9 expression.

Anti-Lamin B1 polyclonal antibody (cat# ab16048, 1:1,000) was "Knock-Out Validated" by vendor Abcam: "To ensure you have highly specific antibodies, we use KO-validation via CRISPR-Cas9 genome-editing, to deliver the reliable results that your research demands."

α/β-Tubulin polyclonal antibody (cat# 2148, 1:1,000) was validated by Western Blot, a single band showed at indicated molecular weight (~55 KDa).

APC conjugated Fetal Hemoglobin Polyclonal Antibody (cat# NB110-41084, 1:2,000) was validated by our previous study by flow cytometry (Qin, K., Huang, P., Feng, R. et al. Publisher Correction: Dual function NFI factors control fetal hemoglobin silencing in adult erythroid cells. Nat Genet 54, 906 (2022). https://doi.org/10.1038/s41588-022-01112-0).

All antibodies listed above have been used and cited by other researchers as showed in manufacturer's website.

Eukaryotic cell lines

Policy information about cell lines and Sex and Gender in Research

Cell line source(s)	EL4, HEK293T, and NK-92 cells were purchased from ATCC. PlatE, MOLM13, and NALM6 were cultured in house.
Authentication	None of the cell lines used were authenticated.
Mycoplasma contamination	All cell lines were tested as mycoplasma negative.
Commonly misidentified lines (See ICLAC register)	No cell lines used in the study are in this database.

Animals and other research organisms

Policy information about studies involving animals; ARRIVE guidelines recommended for reporting animal research, and Sex and Gender in Research

Laboratory animals	TCR transgenic P14 C57BL/6 mice (TCR specific for LCMV DbGP33–41) were bred in house. 6-8 week-old recipient C57BL/6 mice were purchased from NCI. Male and female mice were used.
Wild animals	This study did not involve wild animals.
Reporting on sex	Sex was not considered in this study.
Field-collected samples	The study did not involve samples collected from the field.
Ethics oversight	All mice were used in accordance with Institutional Animal Care and Use Committee (IACUC) guidelines for the University of Pennsylvania.

Note that full information on the approval of the study protocol must also be provided in the manuscript.

Flow Cytometry

Plots

Confirm that:

☒ The axis labels state the marker and fluorochrome used (e.g. CD4-FITC).

☒ The axis scales are clearly visible. Include numbers along axes only for bottom left plot of group (a 'group' is an analysis of identical markers).

☒ All plots are contour plots with outliers or pseudocolor plots.

☒ A numerical value for number of cells or percentage (with statistics) is provided.

Methodology

Sample preparation	For cell lines, samples were directly analyzed by Guava easyCyte HT. For murine in vivo studies, PBMC were isolated from whole blood by histopaque gradient (2000 rpm, 20 min, RT; Histopaque-1083; Sigma). Spleens were mechanically disrupted over a 70 µm filter, followed by ACK lysis. Mouse CD8 T cells were isolated from mouse spleens using EasySep Mouse CD8+ T Cell Isolation Kit (STEMCELL 19853). Human total T cells were isolated from PBMCs from normal donor using EasySep Human T Cell Isolation Kit (STEMCELL 17951). All samples were resuspended in FACS buffer (DPBS + 3% FBS + 2mM EDTA) prior to staining. Cells were stained for 30 min at 4°C (mouse cells) or 20 min at RT (human T cells) followed by washing with FACS buffer. Samples were fixed by Stabilizing Fixative (BD Biosciences 338036) for 15 min at RT and resuspended in FACS buffer for flow cytometry analyses. Frozen G-CSF-mobilized CD34+ HSPCs isolated from the peripheral blood of healthy human donors. At day 13 of the differentiation of CD34+ HSPCs into erythroid cells, 1 million primary erythroid cells were washed with PBS and then fixed with 0.05% glutaraldehyde (Sigma Aldrich, G6257) for 10 minutes. The cells were permeabilized with 0.1% Triton for 3 minutes at room temperature, and then stained with an APC-conjugated HbF antibody (NB110-41084, Novus Biological) for 15 minutes on ice.
Instrument	Millipore Guava easyCyte HT, BD Accuri C6 Plus Flow Cytometer, BD LSRFortessa, BD LSR II, BD FACS ARIA, and BD FACSCanto
Software	FlowJo 10.8.1, BD FACSDiva 8.0.2, and GraphPad Prism 9.4.1
Cell population abundance	The purity of sorted cell population was >90%, which was determined by flow cytometry post sorting.
Gating strategy	For cell lines, live cells were gated by FSC-A/SSC-A, and mCherry negative population or GFP positive population were analyzed. For HSPCs, live cells were gated by FSC-A/SSC-A and singlets were gated by FSC-A/FSC-H, then APC positive population were gated. For primary murine cells, FSC-A/SSC-A was used to gate lymphocytes, and singlets were gated by SSC-A/SSC-H and then FSC-A/FSC-H. Live cells were negative for a LIVE/DEAD stain. CD8+ T cells were identified as CD8+ and negative for CD4 and B220. Total donor P14 cells were distinguished from recipient cells by expression of a distinct congenic marker and CD44. Expression of Vex reporter was next used to identify P14 cells transduced with sgRNA. Finally, expression of the congenic markers CD45.1 and CD45.2 was used to distinguish co-transferred P14 cells from different treatment conditions. For human CAR T cells, FSC-A/SSC-A was used to gate lymphocytes and singlets were gated by FSC-A/FSC-H. Then live cells were gating by negative of LIVE/DEAD dye staining, and CAR19+ (APC+) were further gated. Additional gating was performed as described in figure and supplementary figure legends for individual experiments.

☒ Tick this box to confirm that a figure exemplifying the gating strategy is provided in the Supplementary Information.